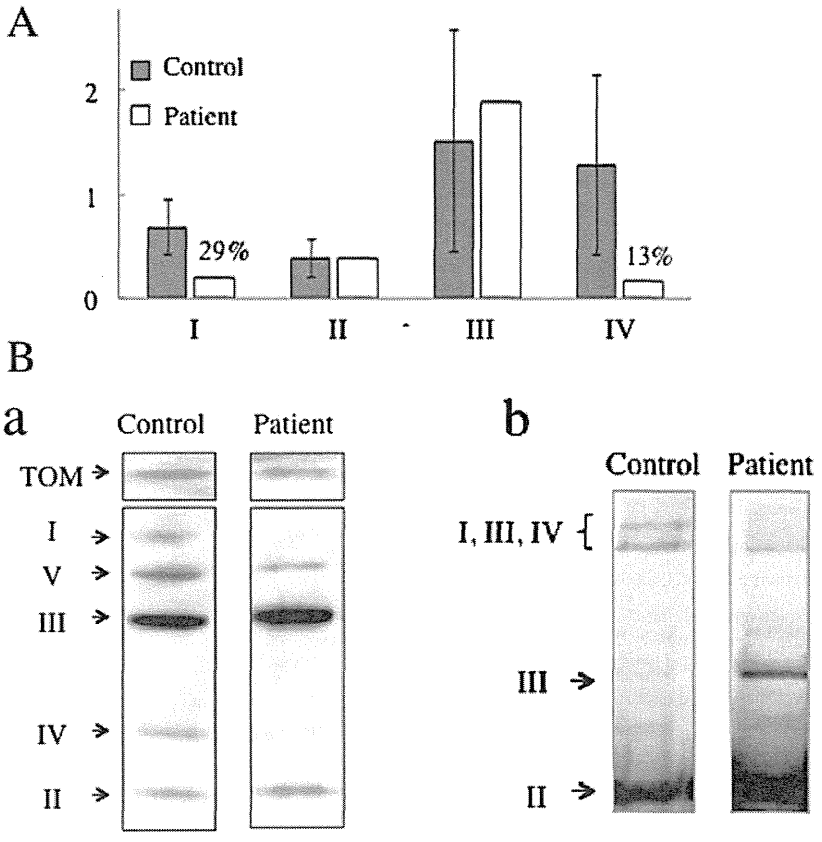

Figure 4 Enzymatic activities of respiratory complexes, and blue native polyacrylamide gel electrophoresis (BN-PAGE) and western blotting for immunodetection. (A) Enzymatic activities of respiratory complexes. Isolated mitochondrial fractions (1 μg protein) of cultured fibroblasts from patient IV-6 and 10 controls were subjected to spectrophotometry. The activity of citrate synthase was used for normalisation. All measurements were performed in triplicate and averaged. The enzymatic activities of complexes I and IV were severely decreased (29% and 13%, respectively). (B). BN-PAGE and western blotting for immunodetection. (a) For the detection of individual complexes, isolated mitochondrial fractions (20 μg protein) were solubilised with 0.5% (w/v) *n*-dodecyl-β-D-maltoside, and then electrophoresed on 3–12% gradient polyacrylamide gels. The subunit-specific primary antibodies used were as follows: NDUFA9 (complex I, Invitrogen) (2.0 μg/ml), SDHA (complex II, Invitrogen) (0.02 μg/ml), UQCRC2 (complex III, Abcam) (0.2 μg/ml), MTCO1 (complex IV, Invitrogen) (0.2 μg/ml), and ATP5B (complex V, Invitrogen) (2.0 μg/ml). Translocase of the outer membrane was used as the loading control. Immunoblot images show that the amounts of complexes I and IV were decreased to about 11% and 21% in patient IV-6. (b) For the detection of supercomplexes, isolated mitochondrial fractions (30 μg protein) were solubilised with 1% (w/v) digitonin, and then electrophoresed on 3–12% gradient polyacrylamide gels. The subunit-specific primary antibodies used were as follows: SDHA (complex II, Invitrogen) (0.02 μg/ml) and UQCRC2 (complex III, Abcam) (0.2 μg/ml). Immunoblot images show that the amounts of supercomplexes that consist of complexes I, III and IV were also reduced to about 30% in patient IV-6.

and peripheral neuropathy. Our patients and SPG7 ones share the symptoms of optic atrophy and neuropathy as well as spastic paraplegia, although the *paraplegin* gene mutation was not identified in this family.

Paraplegin is a nuclear-encoded mitochondrial protein. SPG7 fibroblasts have been demonstrated to exhibit reduced respiratory chain complex I activity.[33] Complex I activity was also reduced in our patient's fibroblasts. Considering the above findings, the present type of HSP has some clinical and biochemical features in common with SPG7. Furthermore, there has been one report of a defect of complex I activity in HSP patients without SPG7 gene mutations,[34] and another one with significant decreases in mitochondrial respiratory chain complexes I and IV in non-SPG4/SPG7 HSP families.[35] These families might have a mutation in the *C12orf65* genes responsible for reduced mitochondrial respiratory chain complex activities.

It may be noteworthy that in Friedreich's ataxia (FA), another nuclear-encoded mitochondrial defect, there is corticospinal degeneration. In rare cases, FA may present clinically as spastic paraparesis.[36 37]

In conclusion, the present study allowed identification of a *C12orf65* gene mutation in AR-HSP with optic atrophy and neuropathy, and revealed a mitochondrial translation dysfunction resulting in reduced enzyme activities of respiratory chain

complexes. Our study should provide additional insights into the pathogeneses of HSPs or other neurodegenerative diseases involving mitochondrial gene mutations.

Acknowledgements We wish to thank Dr Mayumi Komine (Department of Dermatology, Jichi Medical University) for performing the skin biopsy on the patient. We also thank Dr Satoko Kumada (Department of Neuropediatrics, Tokyo Metropolitan Neurological Hospital) and Dr Kazuma Sugie (Department of Neurology, Nara Medical University) for sending the patients' samples.

Contributors HS, YT, JG, ST and YG designed the study; HS, HI, CS, YM, HH, JH, KS, TN, MN, YF and YT performed the experiments; HS, YT, HI, CS, YM, HH, JG, ST and YG collected and analysed the data; HS provided the DNA samples and clinical information; HS, YT, ST and YG wrote the manuscript; and YT, JG, ST, YG and IH provided technical support, conceptual advice and project coordination.

Funding This work was supported by a grant from the Research Committee for Ataxic Diseases (YT and HS) of the Ministry of Health, Labour and Welfare, Japan. This work was also supported by Grants-in-Aid from the Research Committee of CNS Degenerative Diseases (IN and YT), and the Ministry of Health, Labour and Welfare of Japan, and by a Grant-in-Aid for Scientific Research (C) (23591253 to HS) from The Ministry of Education, Culture, Sports, Science and Technology in Japan.

Competing interests None.

Patient consent Obtained.

Ethics approval This study was approved by the institutional review board of the Jichi Medical University, University of Yamanashi, University of Tokyo, and the National Institute of Neuroscience, National Centre of Neurology and Psychiatry.

Provenance and peer review Not commissioned; externally peer reviewed.

Data sharing statement Exome sequencing data are available (DDBJ Sequence Read Archive (DRA) accession number DRA000534).

REFERENCES

1. **Harding AE.** Classification of the hereditary ataxias and paraplegias. *Lancet* 1983;**1**:1151–5.
2. **Hazan J,** Fonknechten N, Mavel D, Paternotte C, Samson D, Artiguenave F, Davoine CS, Cruaud C, Durr A, Wincker P, Brottier P, Cattolico L, Barbe V, Burgunder JM, Prud'homme JF, Brice A, Fontaine B, Heilig B, Weissenbach J. Spastin, a new AAA protein, is altered in the most frequent form of autosomal dominant spastic paraplegia. *Nat Genet* 1999;**23**:296–303.
3. ***Stevanin G,*** Santorelli FM, Azzedine H, Coutinho P, Chomilier J, Denora PS, Martin E, Ouvrard-Hernandez AM, Tessa A, Bouslam N, Lossos A, Charles P, Loureiro JL, Elleuch N, Confavreux C, Cruz VT, Ruberg M, Leguern E, Grid D, Tazir M, Fontaine B, Filla A, Bertini E, Durr A, Brice A. Mutations in SPG11, encoding spatacsin, are a major cause of spastic paraplegia with thin corpus callosum. *Nat Genet* 2007;**39**:366–72.
4. **Salinas S,** Proukakis C, Crosby A, Warner TT. Hereditary spastic paraplegia: clinical features and pathogenetic mechanisms. *Lancet Neurol* 2008;**7**:1127–38.
5. **McDermott CJ,** Grierson AJ, Wood JD, Bingley M, Wharton SB, Bushby KM, Shaw PJ. Hereditary spastic paraparesis: disrupted intracellular transport associated with spastin mutation. *Ann Neurol* 2003;**54**:748–59.
6. **Xia CH,** Roberts EA, Her LS, Liu X, Williams DS, Cleveland DW, Goldstein LS. Abnormal neurofilament transport caused by targeted disruption of neuronal kinesin heavy chain KIF5A. *J Cell Biol* 2003;**161**:55–66.
7. **Tarrade A,** Fassier C, Courageot S, Charvin D, Vitte J, Peris L, Thorel A, Mouisel E, Fonknechten N, Roblot N, Seilhean D, Dierich A, Hauw JJ, Melki J. A mutation of spastin is responsible for swellings and impairment of transport in a region of axon characterized by changes in microtubule composition. *Hum Mol Genet* 2006;**15**:3544–58.
8. **Koppen M,** Metodiev MD, Casari G, Rugarli EI, Langer T. Variable and tissue-specific subunit composition of mitochondrial m-AAA protease complexes linked to hereditary spastic paraplegia. *Mol Cell Biol* 2007;**27**:758–67.
9. **Nolden M,** Ehses S, Koppen M, Bernacchia A, Rugarli EI, Langer T. The m-AAA protease defective in hereditary spastic paraplegia controls ribosome assembly in mitochondria. *Cell* 2005;**123**:277–89.
10. **Pierson TM,** Adams D, Bonn F, Martinelli P, Cherukuri PF, Teer JK, Hansen NF, Cruz P, Mullikin JC, Blakesley RW, Golas G, Kwan J, Sandler A, Fuentes Fajardo K, Markello T, Tifft C, Blackstone C, Ruqarli EI, Langer T, Gahl WA, Toro C For The Nisc Comparative Sequencing Program. Whole-exome sequencing identifies homozygous AFG3L2 mutations in a spastic ataxia-neuropathy syndrome linked to mitochondrial m-AAA proteases. *PLoS Genet* 2011;**7**:e1002325.
11. **Ferreirinha F,** Quattrini A, Pirozzi M, Valsecchi V, Dina G, Broccoli V, Auricchio A, Piemonte F, Tozzi G, Gaeta L, Casari G, Ballabio A, Rugarli EI. Axonal degeneration in paraplegin-deficient mice is associated with abnormal mitochondria and impairment of axonal transport. *J Clin Invest* 2004;**113**:231–42.
12. **Joshita Y,** Atsumi T, Miyatake T. Two siblings with spastic paraplegia, optic atrophy and peripheral neuropathy. *Rinsho Shinkeigaku* 1982;**22**:901–8.
13. **Fukuda Y,** Nakahara Y, Date H, Takahashi Y, Goto J, Miyashita A, Kuwano R, Adachi H, Nakamura E, Tsuji S. SNP HiTLink: a high-throughput linkage analysis system employing dense SNP data. *BMC Bioinformatics* 2009;**10**:121.
14. **Gudbjartsson DF,** Thorvaldsson T, Kong A, Gunnarsson G, Ingolfsdottir A. Allegro version 2. *Nature Genet* 2005;**37**:1015–16.
15. **Barrett MT,** Scheffer A, Ben-Dor A, Sampas N, Lipson D, Kincaid R, Tsang P, Curry B, Baird K, Meltzer PS, Yakhini Z, Bruhn L, Laderman S. Comparative genomic hybridization using oligonucleotide microarrays and total genomic DNA. *Proc Natl Acad Sci USA* 2004;**101**:17765–70.
16. **Mitsui J,** Takahashi Y, Goto J, Tomiyama H, Ishikawa S, Yoshino H, Minami N, Smith DI, Lesage S, Aburatani H, Nishino I, Brice A, Hattori N, Tsuji S. Mechanisms of genomic instabilities underlying two common fragile-site-associated loci, PARK2 and DMD, in germ cell and cancer cell lines. *Am J Hum Genet* 2010;**87**:75–89.
17. **Matsushima Y,** Adan C, Garesse R, Kaguni LS. Drosophila mitochondrial transcription factor B1 modulates mitochondrial translation but not transcription or DNA copy number in Schneider cells. *J Biol Chem* 2005;**280**:16815–20.
18. **Chomyn A,** Meola G, Bresolin N, Lai ST, Scarlato G, Attardi G. In vitro genetic transfer of protein synthesis and respiration defects to mitochondrial DNA-less cells with myopathy-patient mitochondria. *Mol Cell Biol* 1991;**11**:2236–44.
19. **Hayashi JI,** Ohta S, Takai D, Miyabayashi S, Sakuta R, Goto Y, Nonaka I. Accumulation of mtDNA with a Mutation at Position 3271 in tRNALeu(UUR) Gene Introduced from a Melas Patient to HeLa Cells Lacking mtDNA Results in Progressive Inhibition of Mitochondrial Respiratory Function. *Biochem Biophys Res Commun* 1993;**197**:1049–55.
20. **Mimaki M,** Hatakeyama H, Komaki H, Yokoyama M, Arai H, Kirino Y, Suzuki T, Nishino I, Nonaka I, Goto Y. Reversible infantile respiratory chain deficiency: a clinical and molecular study. *Ann Neurol* 2010;**68**:845–54.
21. **Nijtmans LG,** Henderson NS, Holt IJ. Blue Native electrophoresis to study mitochondrial and other protein complexes. *Methods* 2002;**26**:327–34.
22. ***D'Aurelio M,*** Gajewski CD, Lenaz G, Manfredi G. Respiratory chain supercomplexes set the threshold for respiration defects in human mtDNA mutant cybrids. *Hum Mol Genet* 2006;**15**:2157–69.
23. **Trounce LA,** Kim YL, Jun AS, Wallace DC. Assessment of mitochondrial oxidative phosphorylation in patient muscle biopsies, lymphoblasts, and transmitochondrial cell lines. In: Attardi GM, Chomyn A eds. *Methods in enzymology*. Vol. 264. San Diego: Academic Press USA, 1996:484–509.
24. **Antonicka H,** Ostergaard E, Sasarman F, Weraarpachai W, Wibrand F, Pedersen AM, Rodenburg RJ, van der Knaap MS, Smeitink JA, Chrzanowska-Lightowlers ZM, Shoubridge EA. Mutations in C12orf65 in patients with encephalomyopathy and a mitochondrial translation defect. *Am J Hum Genet* 2010;**87**:115–22.
25. **Richter R,** Rorbach J, Pajak A, Smith PM, Wessels HJ, Huynen MA, Smeitink JA, Lightowlers RN, Chrzanowska-Lightowlers ZM. A functional peptidyl-tRNA hydrolase, ICT1, has been recruited into the human mitochondrial ribosome. *EMBO J* 2010;**29**:1116–25.
26. **Smeitink JA,** Elpeleq O, Antonicka H, Diepstra H, Saada A, Smits P, Sasarman F, Vriend G, Jacob-Hirsch J, Shaaq A, Rechavi G, Welling B, Horst J, Rodenburg RJ, van den Heuvel B, Shoubridge EA. Distinct clinical phenotypes associated with a mutation in the mitochondrial translation elongation factor EFTs. *Am J Hum Genet* 2006;**79**:869–77.
27. **Fornuskova D,** Brantova O, Tesarova M, Stiburek L, Honzik T, Wenchich L, Tietzeova E, Hansikova H, Zeman J. The impact of mitochondrial tRNA mutations on the amount of ATP synthase differs in the brain compared to other tissues. *Biochem Biophys Acta* 2008;**1782**:317–25.
28. **Smits P,** Antonicka H, van Hasselt PM, Weraarpachai W, Haller W, Schreurs M, Venselaar H, Rodenburg RJ, Smeitink JA, van den Heuvel LP. Mutation in subdomain G' of mitochondrial elongation factor G1 is associated with combined OXPHOS deficiency in fibroblasts but not in muscle. *Eur J Hum Genet* 2011;**19**:275–9.
29. **Smits P,** Saada A, Wortmann SB, Heister AJ, Brink M, Pfundt R, Miller C, Haas D, Hantschmann R, Rodenburg RJ, Smeitink JA, van den Heuvel LP. Mutation in mitochondrial ribosomal protein MRPS22 leads to Cornelia de Lange-like phenotype, brain abnormalities and hypertrophic cardiomyopathy. *Eur J Hum Genet* 2011;**19**:394–9.
30. **Abramov AY,** Smulders-Srinivasan TK, Kirby DM, Acin-Perez R, Enriquez JA, Lightowlers RN, Duchen MR, Turnbull DM. Mechanism of neurodegeneration of neurons with mitochondrial DNA mutations. *Brain* 2010;**133**:797–807.
31. **Park SH,** Zhu PP, Parker RL, Blackstone C. Hereditary spastic paraplegia proteins REEP1, spastin, and atlastin-1 coordinate microtubule interactions with the tubular ER network. *J Clin Invest* 2010;**120**:1097–110.
32. **Zuchner S,** Wang G, Tran-Viet KN, Nance MA, Gaskell PC, Vance JM, Ashley-Koch AE, Pericak-Vance MA. Mutations in the novel mitochondrial protein REEP1 cause hereditary spastic paraplegia type 31. *Am J Hum Genet* 2006;**79**:365–9.
33. **Atorino L,** Silvestri L, Koppen M, Cassina L, Ballabio A, Marconi R, Langer T, Casari G. Loss of m-AAA protease in mitochondria causes complex I deficiency and increased sensitivity to oxidative stress in hereditary spastic paraplegia. *J Cell Biol* 2003;**163**:777–87.
34. **Piemonte F,** Casali C, Carrozzo R, Schagger H, Patrono C, Tessa A, Tozzi G, Cricchi F, Di Capua M, Siciliano G, Amabile GA, Morocutti C, Bertini E, Santorelli FM.

Respiratory chain defects in hereditary spastic paraplegias. *Neuromuscul Disord* 2001;**11**:565–9.

35. **McDermott CJ,** Taylor RW, Hayes C, Johnson M, Bushby KM, Turnbull DM, Shaw PJ. Investigation of mitochondrial function in hereditary spastic paraparesis. *Neuroreport* 2003;**14**:485–8.

36. **Castelnovo G,** Biolsi B, Barbaud A, Labauge P, Schmitt M. Isolated spastic paraparesis leading to diagnosis of Friedreich's ataxia. *J Neurol Neurosurg Psychiatry* 2000;**69**:693.

37. **Wilkinson PA,** Bradley JL, Warner TT. Friedreich's ataxia presenting as an isolated spastic paraparesis. *J Neurol Neurosurg Psychiatry* 2001;**71**:707–10.

Sleep Medicine 13 (2012) 102–106

Contents lists available at SciVerse ScienceDirect

Sleep Medicine

journal homepage: www.elsevier.com/locate/sleep

Brief Communication

Preclinical substantia nigra dysfunction in rapid eye movement sleep behaviour disorder

Masayuki Miyamoto [a,*], Tomoyuki Miyamoto [a], Masaoki Iwanami [a], Shin-ichi Muramatsu [b], Sayaka Asari [b], Imaharu Nakano [b], Koichi Hirata [a]

[a] Department of Neurology, Centre of Sleep Medicine, Dokkyo Medical University School of Medicine, Tochigi, Japan
[b] Division of Neurology, Department of Medicine, Jichi Medical University, Tochigi, Japan

ARTICLE INFO

Article history:
Received 10 November 2010
Received in revised form 22 January 2011
Accepted 17 March 2011
Available online 26 October 2011

Keywords:
REM sleep behaviour disorder
6-[^{18}F] Fluoro-meta-tyrosine (FMT) positron emission tomography
Transcranial sonography
Dopaminergic neurons
Parkinson's disease
Substantia nigra hyperechogenicity

ABSTRACT

Objectives: Transcranial sonography (TCS) has been shown to reveal hyperechogenicity of the substantia nigra (SN) in people with Parkinson's disease and in approximately 10% of healthy subjects. It is hypothesized that SN hyperechogenicity in healthy subjects and patients with idiopathic rapid eye movement (REM) sleep behaviour disorder (iRBD) patients is a marker of vulnerability for Parkinson's disease.
Methods: TCS and positron emission tomography (PET) with 6-[^{18}F] fluoro-meta-tyrosine (FMT), which can assess the level of the presynaptic dopaminergic nerve, were performed in 19 male patients with iRBD, mean age 66.4 (standard deviation [SD] 4.9) years, to assess nigrostriatal function.
Results: Nine patients had pathological SN hyperechogenicity (mean age 66.8 [SD 3.9] years; 0.31 [SD 0.12] cm^2) and 10 patients did not have SN hyperechogenicity (mean age 66.0 [SD 5.8] years; 0.11 [SD 0.06] cm^2). FMT uptake at the putamen and caudate was significantly lower in iRBD patients with pathological SN hyperechogenicity compared with those without SN hyperechogenicity. However, no correlation was found between SN echogenicity and FMT uptake. This is in conflict with previous findings which showed that subjects with hyperechogenicity had lower FMT uptake in the striatum.
Conclusion: Pathological hyperechogenic alterations in the SN in patients with iRBD may suggest the existence of preclinical SN dysfunction as determined by FMT-PET.

1. Introduction

Rapid eye movement (REM) sleep behaviour disorder (RBD) is a parasomnia characterised by dream-enacting behaviours, unpleasant dreams and lack of muscle atonia during REM sleep. RBD may be idiopathic or related to neurological disease [1]. Patients with idiopathic RBD (iRBD) have been reported to be at increased risk for developing Parkinson's disease (PD) [2]. Transcranial sonography (TCS) has been shown to reveal hyperechogenicity of the substantia nigra (SN) in patients with PD and in approximately 10% of healthy subjects, and has been suggested as a risk marker for PD in non-Parkinsonian subjects [3]. However, Berg et al. reported that SN hyperechogenicity in the elderly is non-specific and of limited usefulness in predicting an individual's risk for PD [4]. Recently, two case-control studies [5,6] showed that pathological SN hyperechogenicity was significantly more common in patients with iRBD compared to control subjects. iRBD is regarded as one of the non-motor symptoms of PD, and precedes motor symptoms. Schenck et al. identified the development of Parkinsonism in 11 of 29 men initially diagnosed with iRBD [7]. It is hypothesized that SN hyperechogenicity in healthy subjects and patients with iRBD is a vulnerability marker for PD. Although there is strong evidence that the echo originates from increased local iron content, the exact pathophysiological mechanisms for SN hyperechogenicity are not completely understood.

In order to verify the hypothesis that hyperechogenic alterations in the SN may be suggestive of preclinical nigrostriatal dopaminergic dysfunction for patients with iRBD, this study evaluated the presynaptic dopaminergic function in the striatum using 6-[^{18}F] fluoro-meta-tyrosine (FMT) positron emission tomography (PET).

2. Methods

This study was performed in accordance with the Declaration of Helsinki. Procedures were approved by the Ethics Review Committee of Dokkyo Medical University, and informed consent was obtained from each subject. TCS and 6-[^{18}F]FMT PET were performed in 19 males with iRBD confirmed by polysomnography.

* Corresponding author. Address: Dokkyo Medical University School of Medicine, 880 Kitakobayashi Mibu, Tochigi 321-0293, Japan. Tel.: +81 282 87 2152; fax: +81 282 86 5884.
E-mail address: miyamasa@dokkyomed.ac.jp (M. Miyamoto).

1389-9457/$ - see front matter © 2011 Elsevier B.V. All rights reserved.
doi:10.1016/j.sleep.2011.03.024

The mean age of subjects was 66.4 (standard deviation [SD] 4.9) years, the mean estimated duration of RBD was 3.5 (SD 1.8) years, the mean score on the Mini-Mental State Examination (MMSE) was 28.4 (SD 2.0), and the mean score on the Unified Parkinson's Disease Rating Scale (UPDRS) part III was 0.9 (SD 1) (range 0–3). Subjects were recruited from a sleep disorders clinic at Dokkyo Medical University Hospital between July 2008 and 2010. All had a history of recurrent dream-enacting behaviours, and RBD was diagnosed according to the International Classification of Sleep Disorders, second edition [8].

2.1. 6-[^{18}F] Fluoro-meta-tyrosine positron emission tomography

The PET radiotracer FMT is a substrate of the dopamine-synthesizing enzyme. Most FMT signals result from tracer that has been metabolized by aromatic amino acid decarboxylase (AADC) and monoamine oxidase-A, and is trapped in axon terminals as 6-fluoro-m-hydrophenylacetic acid without being released or further processed. FMT signals represent the extent of AADC activity more fully [9,10].

For 6-[^{18}F]FMT PET, the subject was placed on the scanner bed in a GEMINI-TF64 (Philips, Amsterdam, The Netherlands) in the supine position. 6-[^{18}F]FMT (weight × 0.12 mCi) was injected intravenously using a syringe pump. Carbidopa pretreatment was used (weight × 2.5 mg). A 10-min static scan was obtained 80 min following injection of 6-[^{18}F]FMT. 6-[^{18}F]FMT PET and magnetic resonance imaging (MRI) scans were fused using a Putamen Analyzer (WebNet Technology, Nasushiobara, Japan). Regions of interest were placed manually at the perimeters of the right/left putamen, caudate and cerebellum in MRI scans of the same subjects. Right/left putamen:cerebellum (putamen) or caudate:cerebellum (caudate) ratios of 6-[^{18}F]FMT-derived radioactivity were estimated. The sizes of the regions of interest were not fixed. Tissue concentrations of 6-[^{18}F]FMT-derived radioactivity (in mCi/cc) were adjusted for the dose per unit of body mass and expressed in units of mCi-kg/cc-mCi (Fig. 1A and B).

2.2. Transcranial sonography

TCS was performed using a conventional transcranial Doppler sonograph equipped with a 2.5-MHz phased-array transducer as described previously [5]. Hyperechogenic areas on both sides were analysed separately. To compare areas of echogenicity and the frequency of hyperechogenicity, the side of the midbrain (right or left) with the greater area of SN echogenicity in each subject was used for these statistical comparisons. Planimetric quantification of the areas of increased echogenicity was done on both sides of the SN independently (Fig. 1C and D). In accordance with previously reported cut-off values, areas of echogenicity <0.20 cm^2 were classified as normal, and areas of echogenicity $\geq$0.20 cm^2 were classified as pathological [3].

The mean interval between performance of TCS and FMT-PET was 126.6 (SD 174.8) days. TCS is performed routinely to assess preclinical condition at the study institute. Berg et al. reported that the echogenic area of the SN did not change in the course of PD during a 5-year follow-up study [11]. Therefore, the interval between the performance of TCS and FMT-PET cannot be considered to influence the results.

Clinical examinations, including the MMSE and UPDRS, FMT-PET and TCS were performed independently by physicians who were blinded to the results of other examinations.

2.3. Statistical analysis

Values are expressed as mean (SD). *p*-values were determined using the Mann–Whitney *U*-test. A *p*-value <0.05 was taken to indicate statistical significance. A statistical comparison of factors such as age of patients, MMSE score, UPDRS part III score and 6-[^{18}F]FMT uptake was performed between the groups of patients with iRBD based on the presence or absence of pathological SN hyperechogenicity. The Spearman's correlation coefficient was used for analysis of the correlation between the echogenic area of the SN and the degree of 6-[^{18}F]FMT uptake.

3. Results

Demographic and clinical data on patients with iRBD are summarized in Table 1. Nine of the patients with iRBD had pathological SN hyperechogenicity (mean 0.31 [SD 0.12] cm^2) and 10 did not have SN hyperechogenicity (mean 0.11 [SD 0.06] cm^2). Therefore, the 19 patients were divided into two groups: those with and those without SN hyperechogenicity. Age distributions, MMSE scores, and UPDRS part III scores did not differ significantly between the groups. Evaluation of motor activity using the UPDRS part III score ranged from zero to three points, which did not fulfill the diagnostic criteria for probable PD. Compared with the patients without SN hyperechogenicity, the patients with SN hyperechogenicity had significantly lower uptake of 6-[^{18}F]FMT in the putamen (mean 4.40 [SD 0.83] and 3.22 [SD 0.98], respectively; $p = 0.027$) and the caudate (mean 3.69 [SD 0.42] and 2.86 [SD 0.82], respectively; $p = 0.014$) (Table 1). However, the echogenic area of the SN did not correlate with the degree of 6-[^{18}F]FMT uptake in the putamen ($r = -0.4465$, $p = 0.0553$) or the caudate ($r = -0.4007$, $p = 0.0891$). In addition, the UPDRS part III scores did not correlate with the degree of 6-[^{18}F]FMT uptake in the putamen ($r = -0.240$, $p = 0.323$), the caudate ($r = -0.040$, $p = 0.871$), or the echogenic area of the SN ($r = -0.216$, $p = 0.375$).

4. Discussion

Unger et al. [12] identified a significant association between midbrain hyperechogenicity and iRBD, and reported that two out of five iRBD patients with SN hyperechogenicity had unremarkable findings by presynaptic dopamine transporter imaging with fluoropropyl-carbomethoxy-iodophenyl-tropane (FP-CIT) single-photon emission computed tomography (SPECT). Iranzo et al. [13] recently reported that ^{123}I-FP-CIT striatal binding did not correlate with the extent of SN echogenicity in patients with iRBD. In the present study, FMT uptake in the putamen and caudate was significantly lower in iRBD patients with pathological SN hyperechogenicity than in those without SN hyperechogenicity. In contrast to the present results, Iranzo et al. [13] found that patients with SN hyperechogenicity did not have lower tracer uptake compared with patients without SN hyperechogenicity and they did not find a correlation between SN size and tracer uptake.

Booij et al. [14] reported that motor signs of PD started when the decrease in the percentage of ^{123}I-FP-CIT binding ratios in the putamen was 46–64% using age-corrected data. Spiegel et al. [15] and Doepp et al. [16] reported a lack of correlation between SN echogenicity and striatal FP-CIT uptake in patients with PD. Spiegel et al. [15] hypothesized that the pathogenic substrate of SN hyperechogenicity is different from that associated with degeneration of dopaminergic SN projection neurons. Berg et al. [11] failed to find evidence of an increase in the size of the echogenic SN area in a 5-year longitudinal study on PD patients with substantial progression of motor symptoms.

On the other hand, Weise et al. [17] reported a significant correlation between the extension of the echogenic SN area and striatal β-CIT binding. They discussed the possibility that the extension of SN echogenicity may be a consequence of degeneration of dopaminergic neurons in the SN, rather than an independent and

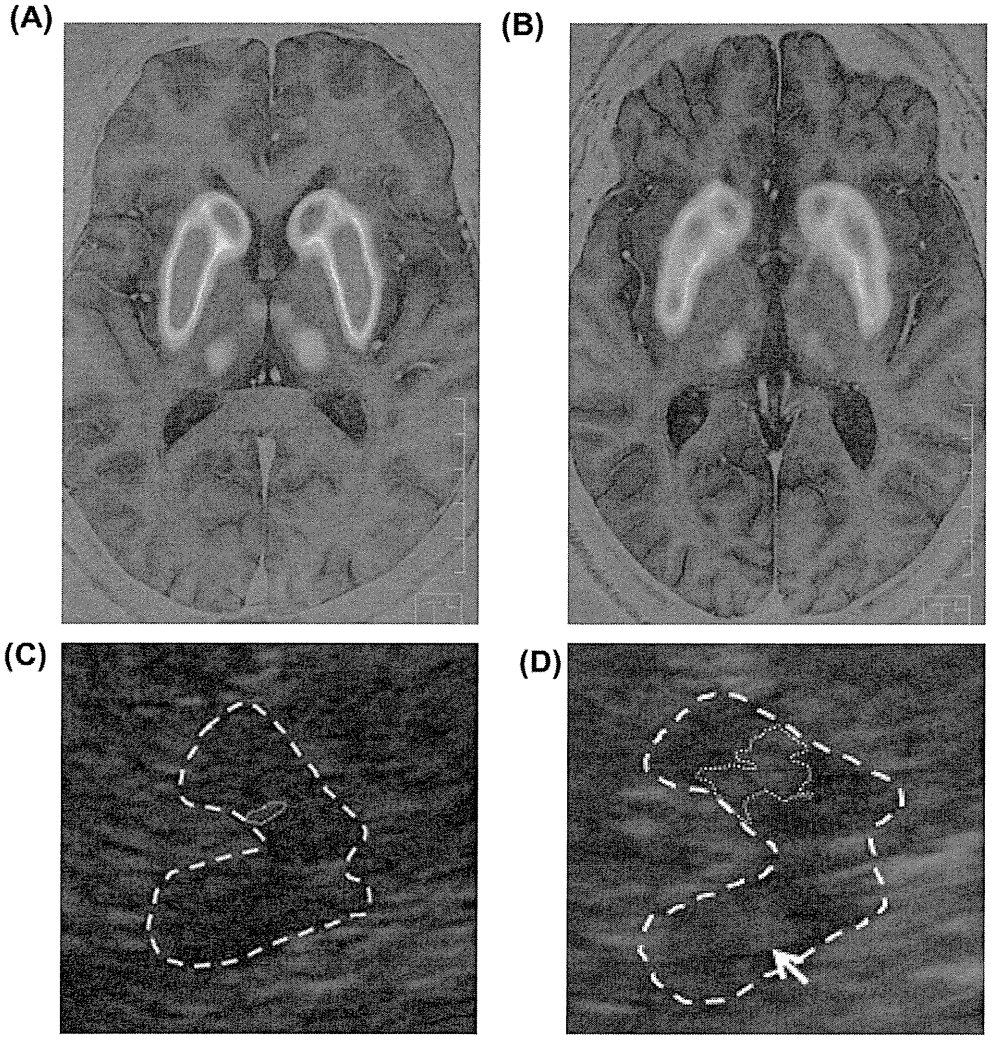

Fig. 1. (A) 6-[^{18}F] Fluoro-meta-tyrosine positron emission tomography (6-[^{18}F]FMT PET) on magnetic resonance imaging (MRI). This demonstrates preserved dopamine terminals in the caudate and putamen in a healthy subject. (B) 6-[^{18}F]FMT PET on MRI. This demonstrates patchy decreased dopamine terminals in the caudate and putamen in a patient with idiopathic rapid eye movement sleep behaviour disorder (iRBD). (C) Transcranial sonography (TCS) of bilateral substantia nigra (SN) hyperechogenicity in a healthy subject. The area of hyperechogenic SN signal within the hypo-echogenic crus cerebri is encircled on the ipsilateral side for planimetric measurement (0.10 cm^2). (D) TCS of bilateral SN hyperechogenicity in a patient with iRBD. The area of the hyperechogenic SN signal within the hypo-echogenic crus cerebri is encircled on the ipsilateral side for planimetric measurement (0.44 cm^2).

Table 1
Area of hyperechogenic substantia nigra (SN) signals in two groups of patients with idiopathic rapid eye movement sleep behaviour disorder (n = 19).

	SN hyperechogenicity*		p-Value
	Normal (<0.20 cm^2) (n = 10)	Pathological (⩾0.20 cm^2) (n = 9)	
Age (years), mean (SD)	66.0 (5.8)	66.8 (3.9)	0.623
Range, years	58–77	62–72	N/A
Sex, male/female	10/0	9/0	N/A
Estimated duration of RBD (years), mean (SD)	3.9 (1.7)	4.3 (2.1)	0.389
MMSE score, mean (SD)	28.4 (2.1)	28.4 (1.9)	0.864
UPDRS part III score, mean (SD)	0.9 (1.1)	1.0 (1.0)	0.729
Uptake of 6-[^{18}F] FMT, mean (SD)			
Putamen	4.40 (0.83)	3.22 (0.98)	0.027
Caudate	3.69 (0.42)	2.86 (0.82)	0.014
Putamen/caudate ratio	1.19 (0.19)	1.12 (0.10)	0.514

RBD, rapid eye movement sleep behaviour disorder; MMSE, Mini-Mental State Examination; UPDRS, Unified Parkinson's Disease Rating Scale; FMT, fluoro-meta-tyrosine; SD, standard deviation; N/A, not applicable.
Transcranial sonography (TCS) was considered pathological when SN echogenicity was ⩾0.20 cm^2.
p-Value was determined by Mann–Whitney U-test.
*Side of the midbrain (right or left) with the greater area of SN echogenicity.

mechanistically unrelated phenomenon. SN echogenicity is sensitive to degeneration of dopaminergic neurons. A report by Behnke et al. [18] showed that ^{18}fluoro-DOPA uptake was lowest in patients with PD, followed by individuals with SN hyperechogenicity, and finally healthy controls without SN hyperechogenicity. The difference was significant between the three groups. Walter et al. [19] reported that brain parenchyma sonography demonstrated SN hyperechogenicity in concordance with abnormal nigrostriatal ^{18}F-DOPA PET in all symptomatic and three asymptomatic *Parkin* mutation carriers. Thus, they suggested SN hyperechogenicity as an early marker for detection of preclinical Parkinsonism. DelleDonne et al. [20] showed that incidental Lewy body disease (ILBD) has nigrostriatal pathological features that are intermediate between those in pathologically normal persons and patients with PD. Among the participants with ILBD, decreased striatal dopaminergic immunoreactivity was documented for both tyrosine hydroxylase and vesicular monoamine transporter 2 in comparison with the pathologically normal subjects; the reductions were even greater in patients with PD. Also, SN neuronal loss correlated with both striatal vesicular monoamine transporter 2 and tyrosine hydroxylase. Thus, ILBD probably represents presymptomatic PD rather than non-specific, age-related α-synuclein pathological changes.

The current study compared FMT-PET findings in patients with iRBD with and without SN hyperechogenicity. Pathological SN hyperechogenicity in iRBD may be suggestive of nigrostriatal dopaminergic dysfunction, as determined by FMT-PET. However, there was no significant correlation between the area of SN hyperechogenicity and the degree of 6-[^{18}F]FMT uptake. It may be that these two parameters have different characteristics. In other words, the area of SN echogenicity is thought to be a stable marker, whereas the uptake of dopaminergic tracer changes progressively with time.

Iranzo et al. found that 19% of 43 patients developed a neurodegenerative syndrome such as PD, dementia with Lewy bodies (DLB), or multiple system atrophy (MSA) 2.5 years after TCS and ^{123}I-FP-CIT SPECT. They postulated that the combined use of ^{123}I-FP-CIT SPECT and TCS is a potential strategy for early identification of patients with iRBD who are at risk for development of a synucleinopathy [13]. They also reported that one case of iRBD who developed MSA had decreased striatal ^{123}I-FP-CIT uptake and normal echogenic SN, and this discrepancy might be explained by the fact that SN hyperechogenicity is less common in MSA than in PD or DLB [13]. Even when SN echogenicity is normal in iRBD, the risk for developing MSA remains. Therefore, patients with iRBD who are at risk for developing not only PD or DLB, but also MSA need to be followed-up.

This study had several limitations. One weak point was that the mean interval between TCS and FMT-PET was approximately four months. Berg et al. reported that the area of SN echogenicity did not change with time in PD [11], but this has not been investigated in patients with iRBD. Due to the lack of a control group in this study, it was not possible to assess if those patients with abnormal PET results had a greater or different echogenic size than those with normal PET results. Satisfactory results of TCS are difficult to obtain in females [5], and all subjects in the study were male. In the future, in order to clarify whether there is a gender difference in the relationship between SN hyperechogenicity and FMT-PET findings, it may be helpful to determine the background of the gender differences in the onset of PD.

Hyperechogenic alterations in the SN may suggest the existence of preclinical SN dysfunction and of an underlying neurodegenerative disorder such as PD or DLB associated with nigrostriatal dysfunction in patients with iRBD. In terms of clinical interest and use of the study findings, there is a need for close clinical follow-up to detect the early signs of a disease characterised by Parkinsonism, and also to test neuroprotective therapies in the near future in such patients.

Financial disclosure

This work was supported by Grants-in-Aid from the Research Committee of CNS Degenerative Diseases, the Ministry of Health, Labour and Welfare of Japan.

Conflict of interest

The ICMJE Uniform Disclosure Form for Potential Conflicts of Interest associated with this article can be viewed by clicking on the following link: doi:10.1016/j.sleep.2011.03.024.

Acknowledgements

The authors wish to thank their colleagues, particularly Y. Inoue (Japan Somnology Centre, Neuropsychiatry Research Institute and Department of Somnology, Tokyo Medical University). The authors also thank Dr. Masaya Segawa (Segawa Neurological Clinic for Children) for reviewing and commenting on the manuscript, and Junichi Saitou and Toshihiko Satou (PET Centre, Utsunomiya Central Clinic) for their technical support in performing FMT-PET.

References

[1] Boeve BF. REM sleep behavior disorder: updated review of the core features, the REM sleep behavior disorder-neurodegenerative disease association, evolving concepts, controversies, and future directions. Ann NY Acad Sci 2009;1184:15–54.
[2] Postuma RB, Lang AE, Massicotte-Marquez J, Montplaisir J. Potential early markers of Parkinson's disease in idiopathic REM sleep behavior disorder. Neurology 2006;66:845–51.
[3] Berg D. Transcranial ultrasound as a risk marker for Parkinson's disease. Mov Disord 2009;24:S677–83.
[4] Berg D, Seppi K, Liepelt I, et al. Enlarged hyperechogenic substantia nigra is related to motor performance and olfaction in the elderly. Mov Disord 2010;25:1464–9.
[5] Iwanami M, Miyamoto T, Miyamoto M, Hirata K, Takada E. Relevance of substantia nigra hyperechogenicity and reduced odor identification in idiopathic REM sleep behavior disorder. Sleep Med 2010;11:361–5.
[6] Stockner H, Iranzo A, Seppi K, et al. Midbrain hyperechogenicity in idiopathic REM sleep behavior disorder. Mov Disord 2009;24:1906–9.
[7] Schenck CH, Bundlie SR, Mahowald MW. Delayed emergence of a parkinsonian disorder in 38% of 29 older men initially diagnosed with idiopathic rapid eye movement sleep behavior disorder. Neurology 1996;46:388–93.
[8] American Academy of Sleep Medicine. International Classification OF Sleep Disorders. 2nd ed. Diagnosis and coding manual. Westcheste, IL: American Academy of Sleep Medicine; 2005. p. 148–52.
[9] Braskie MN, Wilcox CE, Landau SM, et al. Relationship of striatal dopamine synthesis capacity to age and cognition. J Neurosci 2008;28:14320–8.
[10] Muramatsu S, Fujimoto K, Kato S, et al. A phase I study of aromatic L-amino acid decarboxylase gene therapy for Parkinson's disease. Mol Ther 2010;18:1731–5.
[11] Berg D, Merz B, Reiners K, Naumann M, Becker G. Five-year follow-up study of hyperechogenicity of the substantia nigra in Parkinson's disease. Mov Disord 2005;20:383–5.
[12] Unger MM, Möller JC, Stiasny-Kolster K, et al. Assessment of idiopathic rapid-eye-movement sleep behavior disorder by transcranial sonography, olfactory function test, and FP-CIT-SPECT. Mov Disord 2008;23:596–9.
[13] Iranzo A, Lomena F, Stockner H, et al. Decreased striatal dopamine transporter uptake and substantia nigra hyperechogenicity as risk markers of synucleinopathy in patients with idiopathic rapid-eye-movement sleep behaviour disorder: a prospective study. Lancet Neurol 2010;9:1070–7.
[14] Booij J, Bergmans P, Winogrodzka A, Speelman JD, Wolters EC. Imaging of dopamine transporters with [^{123}I]FP-CIT SPECT does not suggest a significant effect of age on the symptomatic threshold of disease in Parkinson's disease. Synapse 2001;39:101–8.
[15] Spiegel J, Hellwig D, Mollers M, et al. Transcranial sonography and [^{123}I]FP-CIT SPECT disclose complementary aspects of Parkinson's disease. Brain 2006;129:118–9.
[16] Doepp F, Plotkin M, Siegel L, et al. Brain parenchyma sonography and ^{123}I-FP-CIT SPECT in Parkinson's disease and essential tremor. Mov Disord 2008;23:405–10.

[17] Weise D, Lorenz R, Schliesser M, Schirbel A, Reiners K, Classen J. Substantia nigra echogenicity: a structural correlate of functional impairment of the dopaminergic striatal projection in Parkinson's disease. Mov Disord 2009;24:1669–75.
[18] Behnke S, Schroeder U, Dillmann U, et al. Hyperechogenicity of the substantia nigra in healthy controls is related to MRI changes and to neuronal loss as determined by F-Dopa PET. NeuroImage 2009;47:1237–43.
[19] Walter U, Klein C, Hilker R, Benecke R, Pramstaller PP, Dressler D. Brain parenchyma sonography detects preclinical parkinsonism. Mov Disord 2004;19:1445–9.
[20] DelleDonne A, Klos KJ, Fujishiro H, et al. Incidental Lewy body disease and preclinical Parkinson disease. Arch Neurol 2008;65:1074–8.

ELSEVIER

Brain & Development 35 (2013) 165–171

BRAIN & DEVELOPMENT
Official Journal of the Japanese Society of Child Neurology

www.elsevier.com/locate/braindev

Original article

Peripheral nerve abnormalities in pediatric patients with spinal muscular atrophy

Takahiro Yonekawa [a], Hirofumi Komaki [a,*], Yuko Saito [b], Kenji Sugai [a], Masayuki Sasaki [a]

[a] *Department of Child Neurology, National Center Hospital, National Center of Neurology and Psychiatry (NCNP), Tokyo, Japan*
[b] *Department of Pathology and Laboratory Medicine, National Center Hospital, National Center of Neurology and Psychiatry (NCNP), Tokyo, Japan*

Received 23 November 2011; received in revised form 14 March 2012; accepted 15 March 2012

Abstract

We examined the specific nerve conduction deficits distinguishing spinal muscular atrophy (SMA) subtypes I and II. Five SMA I patients (age, 0.2–1.1 years) and 10 SMA II patients (age, 1.0–2.8 years) were examined. Patients were compared to age-matched controls for motor and sensory conduction velocity (MCV and SCV) changes, compound muscle and sensory nerve action potential amplitudes (CMAP and SNAP), and F-wave occurrence (FO). Slower MCVs were found in three of five SMA I patients; all five exhibited markedly decreased CMAP amplitudes. Tibial nerve CMAP amplitudes significantly reduced in SMA II patients ($p < 0.01$). Slower SCVs and decreased SNAP amplitudes were observed in three of five SMA I patients but not in SMA II patients. Although FOs were reduced in both extremities of SMA I patients, the reduction was prominent in the tibial nerve of SMA II patients ($p = 0.031$). Loss of motor units may be widespread in the early stage of SMA I, while specific to the legs in young SMA II patients. SMA I showed sensory nerve degeneration, especially of large myelinated fibers. SMA II showed no sensory nerve abnormalities.

Keywords: Spinal muscular atrophy; Nerve conduction study; Peripheral nerve abnormality; Sensory nerve degeneration; Wallerian degeneration

1. Introduction

Spinal muscular atrophy (SMA) is a hereditary disease characterized by degeneration and loss of motor neurons in the spinal cord and brain stem. Three clinical types (SMA I–III) are recognized [1,2]. Spinal muscular atrophy type I patients exhibit weakness before 6 months of age and are unable to sit without support, while SMA II patients usually exhibit weakness by 18 months but are able to sit unsupported at some point in their clinical course. Spinal muscular atrophy type III patients generally have a milder course and are able to walk independently. Patients with marked abnormalities in peripheral sensory nerve conduction are excluded by the diagnostic criteria for infantile SMA, but histological studies have shown loss of myelinated fibers, myelin breakdown, and axonal degeneration in sensory as well as motor nerves of SMA I patients [3–6]. For example, sural nerve biopsy in an eight-year-old SMA II patient revealed mild sensory nerve pathology, including myelin breakdown and myelin ovoids (our unpublished case).

Several studies have analyzed nerve conduction in SMA, but samples sizes were small. Furthermore, there

* Corresponding author. Address: Department of Child Neurology, National Center Hospital, NCNP, 4-1-1, Ogawa-Higashicho, Kodaira, Tokyo 187 8551, Japan. Tel.: +81 42 3412711; fax: +81 42 3462153.
E-mail address: komakih@ncnp.go.jp (H. Komaki).

0387-7604/$ - see front matter © 2012 The Japanese Society of Child Neurology. Published by Elsevier B.V. All rights reserved.
http://dx.doi.org/10.1016/j.braindev.2012.03.009

was considerable variation in age at assessment, which complicates interpretation because the contribution of different axonal types changes during development. Electrophysiological studies have reported reduced motor conduction velocities (MCVs) in some SMA I patients resulting from loss of large myelinated fibers and smaller compound muscle action potential (CMAP) amplitudes in both SMA I and II patients [7,8]. Conversely, two studies found no reduction in sensory nerve conduction velocity in any type of SMA [9,10], although one reported that sural nerve responses were below detection in all SMA I patients [9].

In light of these contradictory results, the aim of the present study is to assess peripheral nerve conduction abnormalities in pediatric SMA patients in a narrow age range and characterize the nerve and axonal subtypes most affected in the different clinical types.

2. Subjects

Written informed consent was obtained from the parents of all patients in accordance with the Declaration of Helsinki for investigations involving human subjects.

Between September 2001 and January 2011, 15 patients aged 0.2–2.8 years were admitted to National Center Hospital, National Center of Neurology and Psychiatry. All were diagnosed with SMA based on clinical history and typical electromyographic patterns. Peripheral blood samples were drawn for genomic DNA analysis of survival of motor neuron 1 (*SMN1*) and neuronal apoptosis-inhibitory protein (*NAIP*). Patients were diagnosed with SMA I or SMA II according to the criteria established by the International SMA Collaboration Workshop of 1990 [1].

3. Methods

3.1. Electrophysiology

This is a retrospective investigation. On admission to our hospital, all patients are evaluated by nerve conduction study (NCS) under drug-induced sleep to confirm or exclude peripheral neuropathy, while the skin temperature is kept higher than 34 °C. Motor and sensory nerve responses were evoked and recorded using an electromyograph (Neuropack Four, Nihon Kohden Co., Tokyo, Japan).

To evoke CMAPs and the F-waves, supramaximal electrical stimuli (0.2–0.3 ms) were delivered through a two-pronged stimulator placed either over the median and ulnar nerve at the wrist and elbow, respectively, or over the posterior tibial nerve at the ankle and popliteal fossa. The F-wave with the shortest latency (F-wave minimal latency) was selected from 20 consecutive (but clearly identified) F-responses. Surface recording electrodes were placed over the main bulk of the thenar, hypothenar, and abductor hallucis muscles for recording CMAPs and F-waves from the median, ulnar, and tibial nerves, respectively. The latency of the CMAPs and F-waves were measured from the stimulus artifact to the initial negative deflection from baseline. The CMAP amplitudes were measured from the negative to the positive peak. Sensory nerve action potentials were evoked by orthodromic stimulation from a ring electrode placed on the second finger for median nerve recording, on the fifth finger for ulnar nerve recording, or by a two-pronged stimulator placed below the lateral malleolus for sural nerve recording. The SNAPs of the sural nerve were recorded by an electrode positioned at a variable surface position depending on the length of the leg. All SNAPs analyzed were the average of approximately 30 responses evoked using supramaximal stimulus intensity. The latency of sensory conduction was measured from the stimulus artifact to the positive peak of the SNAP, and the SNAP amplitude was measured from the positive to the negative peak.

The nerve conduction parameters from SMA I patients (MCV, CMAP, F-wave minimal latency, F-wave frequency, SCV, and SNAP) were compared to those recorded from non-SMA patients less than 1 year of age, while nerve conduction parameters from SMA II patients were compared to controls between 1 and 3 years of age.

3.2. Control patients

We retrospectively investigated NCSs of nine pediatric patients less than a year old (median: 0.8 years, range: 0.3–0.9 years) and 15 patients between 1 and 3 years old (median: 1.5 years, range: 1.1–2.8 years) examined for different disease conditions over the past 4 years. Neuromuscular disorders were excluded in all but two control patients (one patient aged <1 year with congenital muscular dystrophy and another with Duchenne muscular dystrophy).

3.3. Statistical analyses

The two-tailed unpaired group *t*-test was used to compare the mean MCVs, CMAP amplitudes, sensory conduction velocities (SCVs), SNAP amplitudes, and F-wave minimal latencies between SMA II patients and age-matched controls. The Mann–Whitney *U* test was used to compare the medians of F-wave occurrence (% of evoked responses) of SMA II patients and controls. Differences were considered statistically significant at $p < 0.05$. The MCV, CMAP amplitudes, F-wave latency, SCV, and SNAP amplitudes are expressed as mean ± standard deviation (SD).

4. Results

4.1. Genomic analysis of *SMN1* and *NAIP* genes (Table 1)

Nine boys and six girls with confirmed SMA were recruited for the study (Table 1). The median age at diagnosis was 0.3 years for SMA I (range: 0.2–1.1 years) and 1.9 years for SMA II (range: 1.0–2.8 years). Analyses of *SMN1* and *NAIP* genes confirmed the homozygous absence of *SMN1* exons 7 and 8 in all SMA I patients and in all but one (9/10) SMA II patients. This single SMA II patient (Patient 6) exhibited a single *SMN1* exon 8 deletion. Homozygous absence of *NAIP* exons 5 and 6 was confirmed in three SMA I patients but found in no SMA II patient.

4.2. Motor conduction studies

Motor nerve conduction velocities (MCVs) were slower in three of five SMA I patients (Patients 2, 3, and 5) (Fig. 1a), and all SMA I patients exhibited substantially smaller CMAP amplitudes (Fig. 1b). There was no significant difference between the MCVs of SMA II patients and age-matched controls for any of the three nerves tested (Fig. 1c). In contrast, SMA II patients demonstrated significantly lower CMAP amplitudes of the ulnar and tibial nerves compared to the age-matched controls ($p < 0.000$) and a slightly smaller median nerve CMAP amplitude that did not reach statistical significance ($p = 0.107$) (Fig. 1d).

Table 1
Descriptive characteristics of each patient.

Pt	Age at diagnosis (y)	Sex	Subtype	*SMN1*		*NAIP*	
				Exon 7	Exon 8	Exon 5	Exon 6
1	1.1	F	I	del	del	del	del
2	0.2	M	I	del	del	del	del
3	0.3	F	I	del	del	del	del
4	0.8	F	I	del	del	normal	normal
5	0.3	M	I	del	del	normal	normal
6	2.3	F	II	del	1 copy	1 copy	normal
7	1.5	M	II	del	del	normal	normal
8	2.8	M	II	del	del	1 copy	normal
9	1.3	M	II	del	del	normal	normal
10	1.0	M	II	del	del	normal	normal
11	1.8	F	II	del	del	normal	normal
12	2.0	F	II	del	del	normal	normal
13	1.5	M	II	del	del	normal	normal
14	1.9	M	II	del	del	1 copy	normal
15	2.2	M	II	del	del	normal	normal

del, deletion; *NAIP*, neuronal apoptosis-inhibitory protein; Pt, patients; *SMN1*, survival of motor neuron.

4.3. Sensory conduction studies

The SCVs were slower in the median and sural nerves of three SMA I patients (2, 3, and 5) compared to the control group, while no apparent differences in SNAP amplitudes of either median or ulnar nerve were observed (Fig. 1e and f). A comparison of SCVs and SNAPs from SMA II patients and controls showed no statistical differences in either the ulnar or median nerve (Fig. 1g and h).

The SNAP of the sural nerve decreased with increasing distance between the stimulator cathode and recording electrode; therefore, SNAP values were plotted against this distance. Three SMA I patients (2, 3, and 5) exhibited lower SNAP amplitudes than controls (Fig. 2a), while SMA II patients showed no marked difference in sural nerve SNAP amplitude compared to controls over the same range of inter-electrode distance (Fig. 2b).

4.4. F-wave studies

Prolonged F-wave latency was observed in one SMA I patient (Patient 1) and a decreased F-wave occurrence (% of trials) in two SMA I patients (Patients 1 and 2), (Fig. 3a and b). A comparison of F-wave minimal latencies between SMA II and age-matched controls revealed a statistically significant increase only in the ulnar nerve ($p = 0.017$) (Fig. 3c). The FOs in SMA II patients significantly decreased in both the ulnar ($p = 0.018$) and tibial nerves ($p = 0.034$) (Fig. 3d).

4.5. Nerve conduction studies in the control patients

The average MCVs and CMAP amplitudes of controls aged <1 year (SMA I control group) were 40.5 ± 4.9 m/s and 6.8 ± 3.4 mV in the median nerve ($n = 8$), 43.6 ± 6.0 m/s and 43.6 ± 6.0 mV in the ulnar nerve ($n = 8$), and 36.2 ± 4.3 m/s and 13.3 ± 3.7 mV in the tibial nerve ($n = 9$), respectively. In control patients aged between 1 and 3 years (SMA II control group), these MCV and CMAP values were 50.6 ± 6.1 m/s and 7.4 ± 3.3 mV in the median ($n = 11$), 49.2 ± 4.6 m/s and 10.9 ± 2.3 mV in the ulnar ($n = 12$), and 46.7 ± 7.3 m/s and 14.5 ± 6.1 mV in the tibial nerve ($n = 15$), respectively.

The sensory conduction velocities of controls aged <1 year were 40.4 ± 7.0 m/s in the median ($n = 8$) and 38.7 ± 6.6 m/s in the ulnar nerve ($n = 8$), while SNAP amplitudes in these controls were 10.4 ± 9.1 μV in the median and 9.1 ± 9.2 μV in the ulnar nerve. The SCVs of controls aged 1–3 years were 42.9 ± 5.5 m/s in the median ($n = 9$) and 45.6 ± 6.2 m/s in the ulnar nerve ($n = 12$), while SNAP amplitudes in these patients were 21.1 ± 5.4 μV in the median and 13.7 ± 3.9 μV in the ulnar nerve. The SCV of the sural nerve was $45.5 \pm$

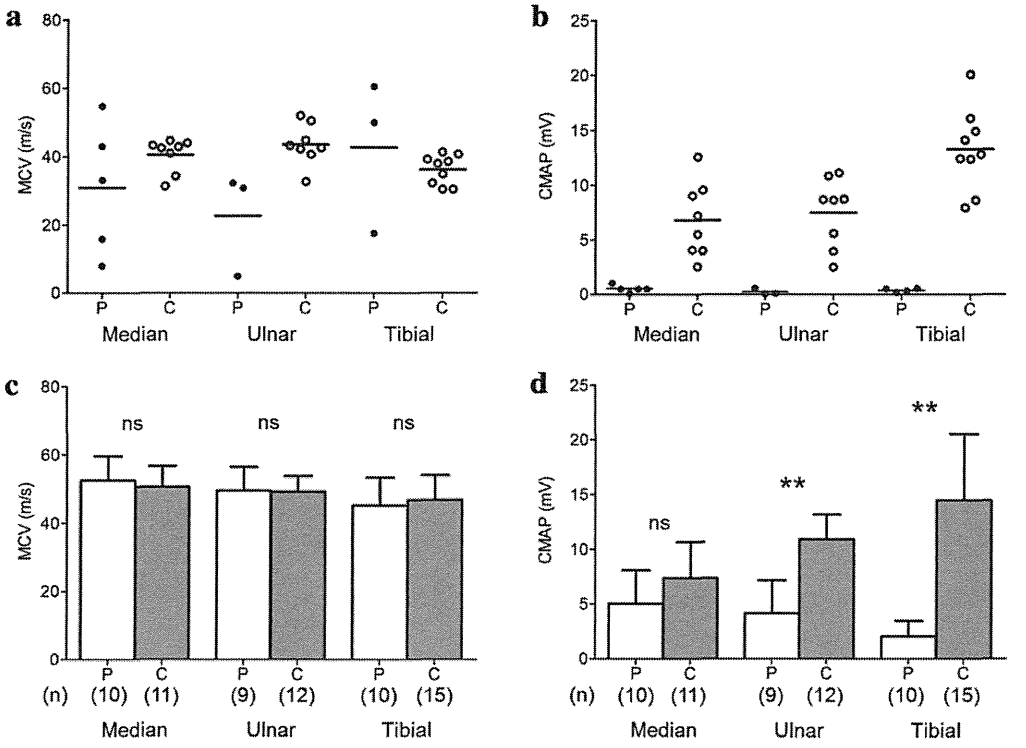

Fig. 1. (a, b) MCV and CMAP values from the ulnar, median, and tibial nerves of SMA I and control patients. Solid lines indicate the means. Three of the SMA I patients show slower MCVs. All five SMA I patients demonstrate decreased CMAP amplitudes in all three nerves. (c, d) Bar graphs comparing MCV (in m/s) and CMAP amplitudes (in mV) between SMA II patients (white) and age-matched control patients (gray). Error bars indicate standard deviations (SDs). (c) There is no statistical differences in mean MCV between SMA II and control patients. (d) CMAPs of the ulnar and tibial nerve were significantly reduced in SMA II patients ($^{**}p < 0.000$). (n): sample number, ns: not significant. (e, f) SCV and SNAP values from SMA I (closed circles) and age-matched control patients (open circles). Solid lines indicate the means. (e) Three SMA I patients show slower conduction velocities of the median and sural nerves, while there are no apparent differences in SNAP amplitudes of the median and ulnar nerves between SMA I and the control patients (f). (g, h) Bar graphs comparing the SCVs and SNAPs of SMA II (white) and control patients (gray). Error bars indicate SDs. No statistical difference are seen in any of the tested nerves. (n): sample number, ns; not significant.

8.3 m/s in controls less than 1 year of age ($n = 8$) and 50.9 ± 9.1 m/s in those aged between 1 and 3 years ($n = 14$). The SNAP amplitudes of the sural nerve depended on the distance between the stimulating cathode and recording electrodes and are presented in scatter plots (Fig. 2). The R values were -0.62 in controls less than 1 year of age ($n = 8$) and -0.47 in those aged between 1 and 3 years ($n = 14$).

The minimum latencies of the F-wave in controls under 1 year of age were 14.4 ± 1.1 ms in the median ($n = 8$), 14.9 ± 0.8 ms in the ulnar ($n = 8$), and 21.5 ± 1.0 ms in the tibial nerves ($n = 9$). The latencies of controls aged between 1 and 3 years were 15.4 ± 1.6 ms in the median ($n = 14$), 15.0 ± 1.5 ms in the ulnar ($n = 13$), and 22.0 ± 2.4 ms in the tibial nerves ($n = 13$). The occurrence of F-waves (FOs, % of trials) in control patients less than 1 year of age and in controls aged between 1 and 3 years are presented in Fig. 3b and d, respectively. Both the mean minimum latency and median occurrence of F-waves were reduced in SMA I patients relative to the controls (Fig. 3a and b); however, the sample size of SMA I patients was small. In SMA II patients, the minimum latency was significantly prolonged in the ulnar nerve. The FO values for each patient were plotted by percentile for F-wave occurrence analysis (Fig. 3d), which revealed that FO was significantly lower in the ulnar and tibial nerves of SMA II patients.

5. Discussion

We assessed the severity of nerve conduction deficits in SMA patients according to clinical type. Patients with SMA I exhibited smaller CMAP amplitudes and decreased F-wave frequencies in all three nerves tested (Figs. 1a and 3b). Similar findings were observed in SMA II, but were especially prominent in the tibial nerve (Figs. 1d and 3d). It is well known that the main pathological changes in SMA involve motor neurons of the anterior spinal horn. The chief electrophysiological findings in patients with motor neuron or axonal degeneration are a decreased maximum CMAP amplitude and but a normal or only minimally reduced MCV [11]. Indeed, SMA II exhibited no significant

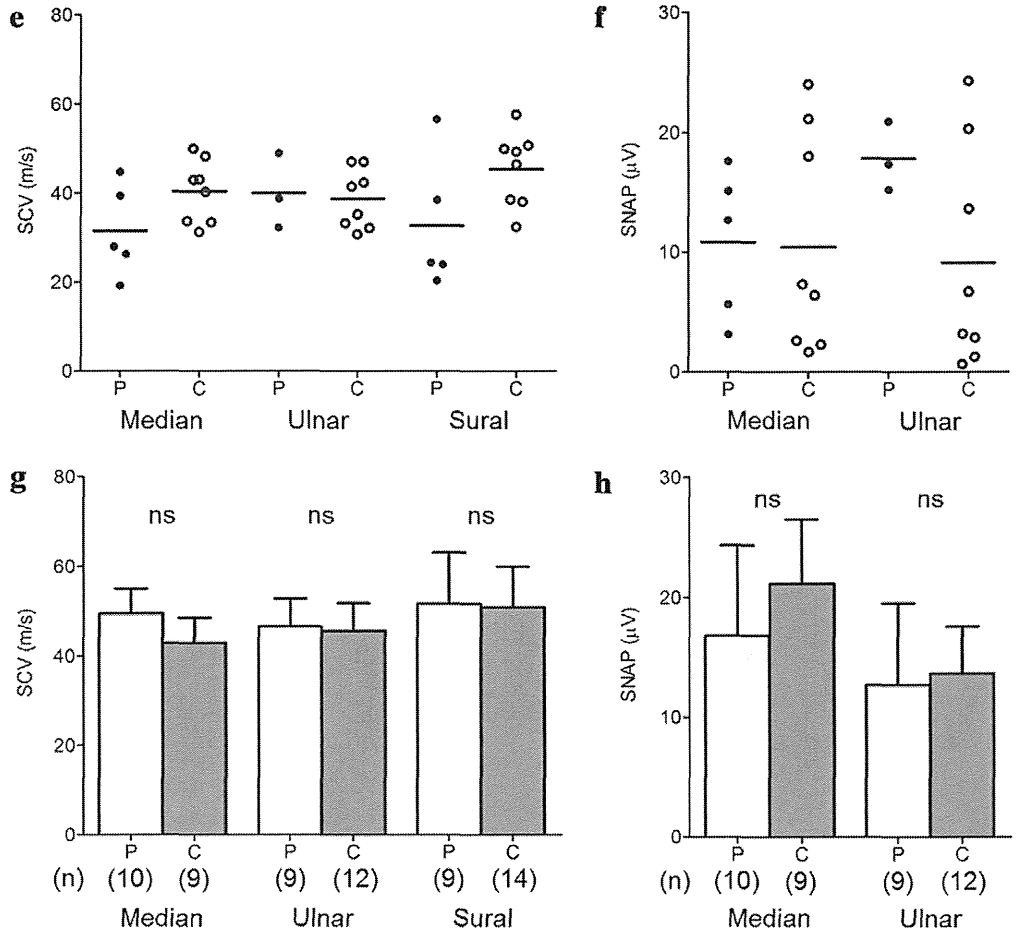

Fig 1. *(continued)*

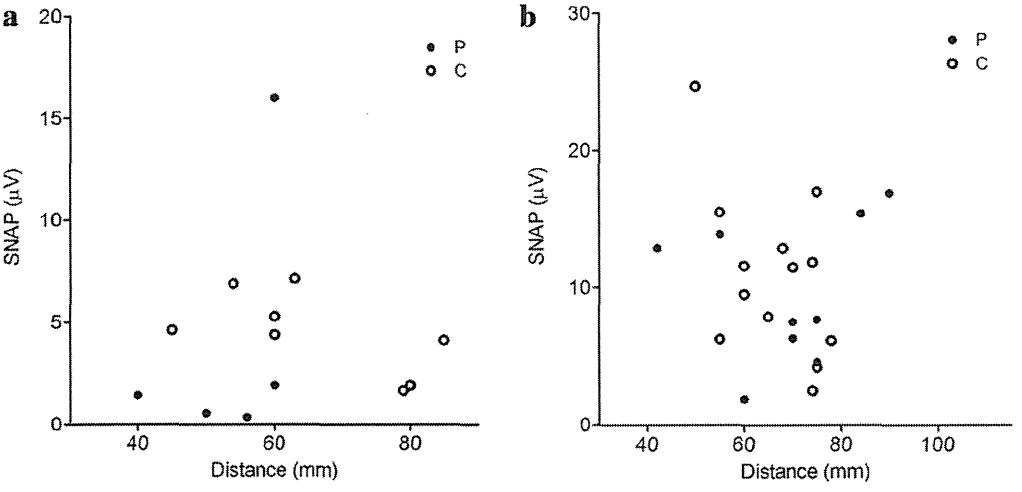

Fig. 2. Scatter plots showing that sural nerve SNAP amplitudes vary with the distance from the stimulating cathode to the distal recording electrode. (a) SMA I and the control patients age <1 year ($R = -0.622$). (b) SMA II and the control patients age 1–3 years ($R = -0.473$). All but one SMA I patient show lower SNAP amplitudes, while SMA II patients exhibit no apparent difference in SNAP distribution compared to controls.

changes in MCV. These results suggest that diffuse loss of ventral horn motor neurons or widespread axonal degeneration occurs at an early stage in SMA I, while these changes occur mainly in the lower extremities of SMA II patients. Slowing of the MCV was also found in three SMA I patients, in accord with several previous

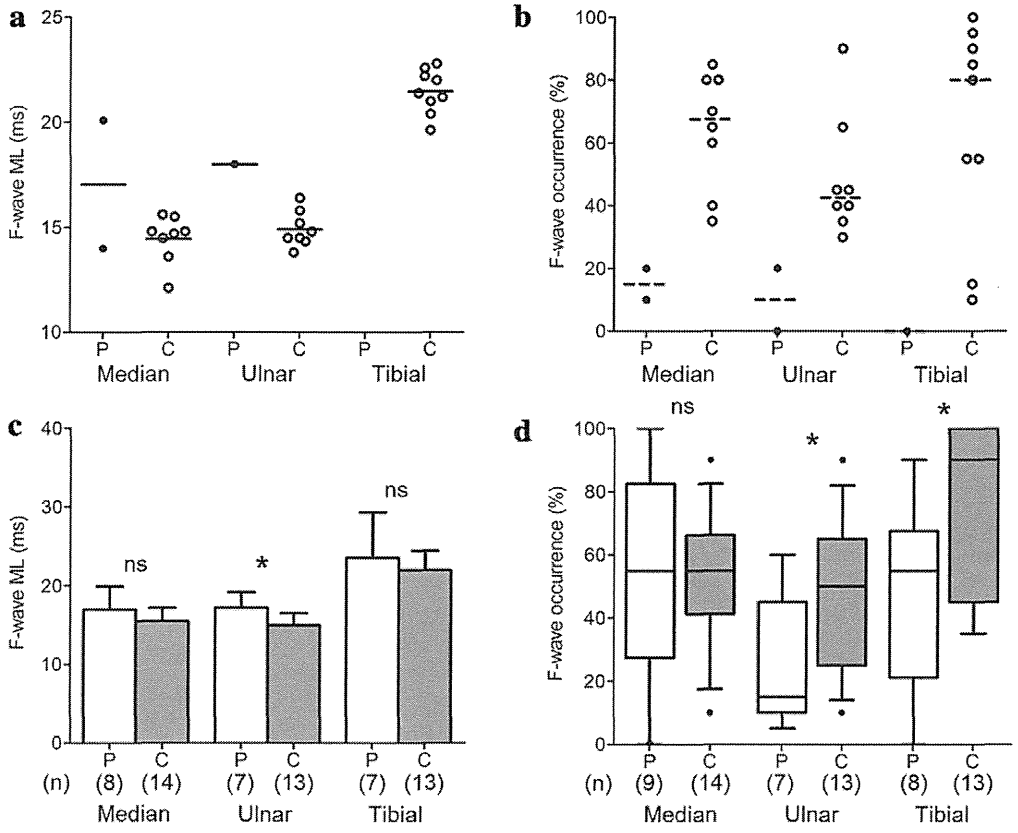

Fig. 3. (a, b) F-wave minimal latency and frequency data of the three nerves in SMA I (filled circles) and control patients (open circles). Solid and dashed lines indicate the means and median. (c) Bar graphs comparing F-wave latencies between SMA II (white) and disease control patients (gray). Error bars indicate SDs. SMA II patients show slow F-wave latencies in the ulnar nerve compared to control patients ($p = 0.013$). (d) Boxplots comparing F-wave frequencies of the three tested nerves between SMA II (white) and control patients (gray). The boxes represent the range from the 25–75th percentile, while the bars span the 10–90th percentile. There is a significant difference (**) between SMA II and the control patients in F-wave frequency of the ulnar ($p = 0.039$) and tibial nerves ($p = 0.031$) by Mann–Whitney U test. (n): sample number, ns; not significant.

studies [7,8,10]. These slower conduction velocities could be caused by demyelination or by loss of fast-conducting myelinated axons, because loss of myelinated peripheral axons can reduce conduction velocity by up to 40% [12]. Chien et al. reported that the number of large myelinated axons was markedly decreased in almost all intramuscular nerve bundles in biopsies of SMA I patients [3]. This reduced MCV in a subpopulation of SMA I patients may reflect loss of spinal motor neurons followed by Wallerian degeneration of axons. In contrast, the normal MCVs in SMA II patients indicate no loss of large diameter myelinated fibers in these patients and suggests that loss is more severe in SMA I patients.

Reduced SNAP amplitude of the sural nerve was observed in all but two SMA I patients (Fig. 2a). Schwartz et al. (1977) did not find measurable sural nerve responses in any of their SMA I patients [9], but the underlying mechanisms were not discussed. Previous reports have shown axonal degeneration of both large and small myelinated fibers of the sural nerve along with signs of Wallerian degeneration [6]. Therefore, it is possible that axonal degeneration can contribute to reduced SNAP amplitudes of the sural nerves. Slower SCVs of the median and sural nerves in some SMA I patients suggest loss of large myelinated fibers in both limbs (Fig. 1e). In contrast, no sensory nerve alterations were reported in histological examinations of sural nerve biopsies [4], and we have encountered only a single case of SMA II with axonal degeneration of the sural nerve (unpublished case). Our SMA II patients showed no apparent difference in SNAP amplitudes compared to control patients (Fig 2b), indicating that SMA II is usually not accompanied by significant degeneration of sensory axons in the sural nerve.

We found significant differences in the pathological progression of SMA I and SMA II. Given that spinal muscular atrophy is a rare genetic disease, this study encompassed a relatively large sample of SMA II patients. In addition, we tested both motor and sensory nerve responses from both the upper and lower extremities and compared these results to well defined age-matched controls. In this study, we included our control patients because they had undergone NCS in the same manner as our SMA patients. However, several limitations should be noted. The sample of SMA I patients was small, which is problematic

because degeneration of large myelinating neurons hinders accurate estimation of conduction parameters. In addition, the distance between recording and stimulating electrodes for sural nerve SNAP amplitude could not be controlled in this retrospective study. Finally, sleep-inducing agents reduce F-wave frequencies, although these agents were applied to both patients and controls. We suggest that the decreased F-wave frequencies in SMA patients reflected axonal degeneration or loss of motor neurons in the anterior horn.

6. Conclusion

In SMA I, the observed reductions in CMAP amplitude and F-wave frequencies in both extremities could reflect diffuse loss of spinal motor neurons. Slower SCVs and reduced SNAP amplitudes suggest that axonal degeneration of sensory nerves, especially large myelinated fibers, can also occur in SMA I. In SMA II, loss of motor neurons was prominent in lower extremities, while no sensory abnormalities were observed.

Acknowledgments

This work was supported by a Grant-in-Aid from the Research Committee of Spinal Muscular Atrophy, the Ministry of Health, Labour and Welfare of Japan, and Intramural Research Grant (23-6) for Neurological and Psychiatric Disorders of NCNP.

References

[1] Munsat TL. Workshop report: International SMA Collaboration. Neuromuscul Disord 1991;1:81.
[2] Zerres K, Rudnik-Schöneborn S. Natural history in proximal spinal muscular atrophy: clinical analysis of 445 patients and suggestions for a modification of existing classifications. Arch Neurol 1995;52:518–23.
[3] Chien YY, Nonaka I. Peripheral nerve involvement in Werdnig–Hoffmann disease. Brain Dev 1989;11:221–9.
[4] Rudnik-Schöneborn S, Goebel HH, Schlote W, Molaian S, Omran H, Ketelsen U, et al. Classical infantile spinal muscular atrophy with SMN deficiency causes sensory neuronopathy. Neurology 2003;60:983–7.
[5] Carpenter S, Karpati G, Rothman S, Watters G, Andermann F. Pathological involvement of primary sensory neurons in Werdnig–Hoffmann disease. Acta Neuropathol 1978;42:91–7.
[6] Marshall A, Duchen LW. Sensory system involvement in infantile spinal muscular atrophy. J Neurol Sci 1975;26:349–59.
[7] Moosa A, Dubowitz V. Motor nerve conduction velocity in spinal muscular atrophy of childhood. Arch Dis Child 1976;51:974–7.
[8] Miyanomae Y, Takeuchi Y, Nishimura A, Kawase S, Hirai K, Ochi M, et al. Motor nerve conduction studies on children with spinal muscular atrophy. Acta Paediatr Jpn 1996;38:576–9.
[9] Schwartz MS, Moosa A. Sensory nerve conduction in spinal muscular atrophies. Dev Med Child Neurol 1977;19:50–3.
[10] Ryniewicz B. Motor and sensory conduction velocity in spinal muscular atrophy. Follow-up study. Electromyogr Clin Neurophysiol 1977;17:385–91.
[11] Kimura J. Basics in nerve conduction study: evoked potentials and electromyography: principles and practice (in Japanese). Tokyo: Igakushoin; 1990.
[12] Gilliatt RW, Hopf HC, Rudge P, Baraiser M. Axonal velocities of motor units in the hand and foot muscles of the baboon. J Neurol Sci 1976;29:249–58.

ELSEVIER

Brain & Development 34 (2012) 213–222

BRAIN & DEVELOPMENT
Official Journal of the Japanese Society of Child Neurology

www.elsevier.com/locate/braindev

Original article

Valproic acid increases *SMN2* expression and modulates SF2/ASF and hnRNPA1 expression in SMA fibroblast cell lines

Indra Sari Kusuma Harahap [a,b], Toshio Saito [c], Lai Poh San [d], Naoko Sasaki [a], Gunadi [a], Dian Kesuma Pramudya Nurputra [a], Surini Yusoff [a], Tomoto Yamamoto [a,e], Satoru Morikawa [a,e], Noriyuki Nishimura [a,e], Myeong Jin Lee [a], Yasuhiro Takeshima [e], Masafumi Matsuo [e], Hisahide Nishio [a,e,*]

[a] *Department of Community Medicine and Social Healthcare Science, Kobe University Graduate School of Medicine, Kobe, Japan*
[b] *Department of Neurology, Faculty of Medicine, Gadjah Mada University, Yogyakarta, Indonesia*
[c] *Department of Neurology, Toneyama National Hospital, Toyonaka, Osaka, Japan*
[d] *Department of Pediatrics, Yong Loo Lin School of Medicine, National University of Singapore, Singapore*
[e] *Department of Pediatrics, Kobe University Graduate School of Medicine, Kobe, Japan*

Received 1 February 2011; received in revised form 14 April 2011; accepted 14 April 2011

Abstract

Spinal muscular atrophy (SMA) is a common autosomal recessive neuromuscular disorder that is caused by loss of the survival motor neuron gene, *SMN1*. SMA treatment strategies have focused on production of the SMN protein from the almost identical gene, *SMN2*. Valproic acid (VPA) is a histone deacetylase inhibitor that can increase SMN levels in some SMA cells or SMA patients through activation of *SMN2* transcription or splicing correction of *SMN2* exon 7. It remains to be clarified what concentration of VPA is required and by what mechanisms the SMN production from *SMN2* is elicited. We observed that in two fibroblast cell lines from Japanese SMA patients, more than 1 mM of VPA increased *SMN2* expression at both the transcript and protein levels. VPA increased not only full-length (FL) transcript level but also exon 7-excluding (Δ7) transcript level in the cell lines and did not change the ratio of FL/Δ7, suggesting that *SMN2* transcription was mainly activated. We also found that VPA modulated splicing factor expression: VPA increased the expression of splicing factor 2/alternative splicing factor (SF2/ASF) and decreased the expression of heterogeneous nuclear ribonucleoprotein A1 (hnRNPA1). In conclusion, more than 1 mM of VPA activated *SMN2* transcription and modulated the expression of splicing factors in our SMA fibroblast cell lines.

1. Introduction

Spinal muscular atrophy (SMA) is a common autosomal recessive neuromuscular disorder characterized by progressive muscular atrophy of the limbs and trunk, resulting from degeneration of α-motor neurons in the spinal cord. The incidence of the disease is approximately 1 in 6,000 live births, and the carrier frequency is 1/40–1/50 [1]. SMA can be classified into three groups: SMA type I (Werdnig–Hoffman disease; severe form), SMA type II (intermediate form) and SMA type III (Kugelberg–Welander disease; mild form) [2]. This classification is based on the age of onset and the achievement of motor milestones. The gene responsible for SMA is the survival motor neuron (*SMN*), which is present as two highly homologous copies within the SMA gene region on chromosome 5q11.2–13.3: telomeric *SMN* (*SMN1*) and centromeric *SMN* (*SMN2*) [3–6].

* Corresponding author at: Department of Community Medicine and Social Healthcare Science, Division of Epidemiology, 7-5-1 Kusunoki-cho, Chuo-ku, Kobe 650-0017, Japan. Tel.: +81 78 382 5540; fax: +81 78 382 5559.
E-mail address: nishio@med.kobe-u.ac.jp (H. Nishio).

0387-7604/$ - see front matter © 2011 The Japanese Society of Child Neurology. Published by Elsevier B.V. All rights reserved.
doi:10.1016/j.braindev.2011.04.010

SMN1 and *SMN2* are identical apart from several nucleotide differences. There is a single nucleotide change in the coding region: nucleotide +6 in exon 7 is C in *SMN1* and T in *SMN2*. However, *SMN1* and *SMN2* encode the same protein, because the nucleotide change is synonymous. *SMN1* is homozygously deleted or interrupted in more than 95% of SMA patients [7,8], and deleteriously mutated in the remaining patients [9–11]. Although it encodes the same protein, *SMN2* does not fully compensate for the loss or dysfunction of *SMN1*. In addition, *SMN2* is deleted in approximately 5% of normal individuals [6]. Based on these findings, *SMN1*, but not *SMN2*, has been recognized as the SMA-causing gene.

Interestingly, *SMN2* has never been reported as absent in SMA patients. In addition, the *SMN2* copy number correlates inversely with the disease severity: a higher *SMN2* copy number may ameliorate the clinical phenotype [1,12]. Accordingly, a study using SMA model mice reported that increased copies of *SMN2* could rescue embryonic lethality in mice, indicating modulation of phenotypic severity [13]. Thus, it is thought that *SMN2* may compensate for the loss of *SMN1* to some degree by modifying the severity of the disease through the production of a small amount of functional SMN protein. Increased expression of *SMN2* thus may provide a treatment strategy for SMA, for which there is currently no effective therapy.

SMN1 and *SMN2* show different splicing patterns. All *SMN1*-derived transcripts contain exon 7, i.e., the full-length *SMN* transcript (FL-*SMN* transcript), while the majority of *SMN2*-derived transcripts lack exon 7 (Δ7-*SMN* transcript), because the C–T change in *SMN2* at nucleotide position +6 in exon 7 induces exon skipping [14,15]. In *SMN1*, a heptamer sequence motif including the C at nucleotide position +6 in exon 7 forms a splicing factor 2/alternative splicing factor (SF2/ASF) binding site as an exonic splicing enhancer (ESE) leading to exon 7 inclusion [16–18]. Meanwhile, the corresponding T nucleotide in *SMN2* disrupts the ESE motif and forms a heterogeneous nuclear ribonucleoprotein A1 (hnRNPA1) binding site as an exonic splicing silencer (ESS), leading to exclusion of exon 7 [19].

Two SMA treatment strategies targeting *SMN2* have been proposed. The first strategy involves splicing correction which would prevent exon 7 skipping in *SMN2*, thus facilitating the inclusion of exon 7 in the *SMN2* mRNA. Several pharmacological compounds and synthetic nucleotides have been reported as suitable for the first strategy. These pharmacological compounds include aclarubicin (known as an anthracycline antibiotic) [20], sodium vanadate (a phosphatase inhibitor) [21], hydroxyurea (a cell cycle inhibitor) [22] and salbutamol (a β2-adrenoceptor agonist) [23–25]. The synthetic nucleotides are termed ESSENCE (exon-specific silencing enhancement by small chimeric effectors) [16], TOES (targeted oligonucleotide enhancers of splicing) [26] and antisense oligonucleotides masking exonic splicing suppressors [27–29]. Recently, a tetracycline-like compound, PTK-SMA I, has been identified as an alternative to synthetic nucleotides in stimulating splicing of exon 7 [30]. The second strategy is through the activation of *SMN2* transcription. Drugs known to activate *SMN2* transcription are interferons [31] and histone deacetylase (HDAC) inhibitors. HDAC inhibitors which have been reported to activate *SMN2* transcription include sodium butyrate [32], valproic acid (VPA) [33,34], phenylbutyrate [35], benzamide M344 [36], suberoylanilide hydroxamic acid (SAHA) [37], Trichostatin A (TSA) [38] and hydroxamic acid LBH589 [39]. Among these HDAC inhibitors, sodium butyrate, benzamide M344 and VPA are also able to indirectly correct the splicing abnormality, mainly through the upregulation of splicing factors.

VPA has been approved by the U.S. Food and Drug Administration and is already widely used for the treatment of epileptic patients. Some studies have shown that VPA increases the expression of FL-*SMN2* transcript [33,34]. According to Brichta et al., VPA may activate the *SMN2* promoter and correct abnormal splicing of *SMN2* exon 7 in SMA fibroblasts [33]. However, some patients did not respond to VPA treatment at the normal dose given to epileptic patients [40,41]. In this study, we determined the effect of VPA dose on *SMN2* expression in fibroblasts from two Japanese SMA patients. In addition, we also demonstrated changes in two trans-acting splicing factors, SF2/ASF and hnRNPA1, which regulate the splicing of *SMN1* and *SMN2* exon 7.

2. Materials and methods

2.1. Cell culture and VPA treatment

Fibroblast cell lines from a type I SMA patient (OK11, skin biopsy at 10 months old, passage 3–10), a type II SMA patient (AM21, skin biopsy at 25 years old, passage 3–10) were used in this study. Both SMA cell lines are deleted for *SMN1*. OK11 cells carry two copies of *SMN2*, and AM21 cells carried three copies of *SMN2*. In the control cells (CO31), two copies of *SMN1* and *SMN2* are present respectively. These fibroblast cell lines were maintained in Dulbecco's Modified Eagle's medium (Sigma–Aldrich, St.Louis, MO) containing 100 U/ml penicillin, 100 μg/ml streptomycin and 10% heat-inactivated fetal bovine serum (Biological Industries, Haemek, Israel) in a 5% CO_2 atmosphere at 37 °C. VPA (Sigma–Aldrich, St. Louis, MO) was dissolved in aqua dest and was freshly prepared before each use [37]. For the dose-dependency experiment, the fibroblasts were incubated with VPA

at final concentrations of 0 (mock), 0.05, 0.5, 1 and 10 mM for 16 h in a 5% CO_2 atmosphere at 37 °C. This optimal time was established in previous experiment [33].

This study was approved by the ethical committee of Kobe University, and inform consent was obtained from the patients and/or their parents.

2.2. Cell viability assay

To evaluate the cell viability and cytotoxicity of VPA, the 3-(4,5-dimethylthiazol-2-yl)-5-(3-carboxymethoxyphenyl)-2-(4-sulfophenyl)-2H-tetrazolium (MTS) assay was performed. The cytotoxic effect of 10 mM VPA was studied using OK11 fibroblasts. One hundred microliters of the cell suspension (1×10^5 cells/ml) was placed in the wells of a 96-well culture dish (Iwaki, Chiba, Japan) and incubated in a 5% CO_2 atmosphere at 37 °C. When the cells reached 90% confluency, VPA was added to each well. The final concentration of VPA in the assay was 10 mM. The cell viabilities 2, 4, 8, 16 and 24 h after the addition of VPA were determined using a CellTiter 96 Aqueous One Solution Cell Proliferation Assay Kit (Promega, Madison, WI) which measures the conversion of MTS to violet formazan by dehydrogenases in metabolically active, proliferating cells.

2.3. RNA extraction and cDNA synthesis

Total RNA was isolated from fibroblast cultures in 6-well plates using Sepasol RNA I reagent (Nacalai Tesque, Kyoto, Japan) according to the manufacturer's protocols. After DNase treatment with DNaseI Amplification Grade (Invitrogen, Carlsbad, CA), total RNA was denatured for 10 min at 65 °C and chilled on ice. Reverse transcription was performed at 55 °C for 30 min in a total volume of 20 μl containing 1 μg of total RNA, 60 μM of random hexamer primers, 1 mM dNTPs, 50 mM Tris/HCl, 30 mM KCl, 8 mM $MgCl_2$ pH 8.5, 20 U of protector RNase inhibitor and 10 U of Transcriptor reverse transcriptase (Roche Diagnostics GmbH, Mannheim, Germany).

2.4. Development of a method for quantification of SMN and splicing factor gene transcript levels

To assess whether VPA is able to influence SMN transcript and protein expression, we treated three passages from each of the two *SMN1*-deleted fibroblast cell lines and the control cell line (OK11, AM21 and CO31, respectively) for 16 h with different concentrations of VPA ranging from 0.05 to 10 mM. After reverse transcription of RNA extracted from the fibroblasts, *SMN* and splicing factor gene transcript levels were determined by quantitative real-time PCR (qRT-PCR).

2.5. Quantitative real-time PCR

qRT-PCR was performed on a LightCycler 1.5 instrument (Roche Diagnostics GmbH, Mannheim, Germany) using FastStart DNA Master SYBR Green I (Roche Diagnostics GmbH, Mannheim, Germany). To evaluate the total transcript levels of the SMN genes, we amplified cDNA fragments encompassing SMN exons 1, 2a and 2b. The FL-SMN and Δ7-SMN transcript levels were quantitated from the levels of the products encompassing SMN exons 7 and 8, and SMN exons 5, 6 and 8, respectively. We used glyceraldehyde-3-phosphate dehydrogenase (*GAPDH*) as an endogenous reference gene, and the levels of *SMN* were expressed relative to those of *GAPDH*.

The primers for the FL-*SMN* and Δ7-*SMN* transcripts have been described previously [36]. For the amplification of total-*SMN* transcripts, the primers were designed to bind in *SMN* exon 1 (5′-GCT ATG GCG ATG AGC AGC GGC-3′) and *SMN* exon 2b (5′-GTT GTA AGG AAG CTG CAG TA-3′). *GAPDH* was amplified using primers in exon 2/3 (5′-GAG TCA ACG GAT TTG GTC GT-3′) and exon 4 (5′-GAC AAG CTT CCC GTT CTC AG-3′).

Conditions for all PCRs were optimized regarding the primer concentration, $MgCl_2$ concentration and annealing temperatures. A mastermix of the following reaction components was prepared at the indicated final concentration: 9.4 μl of water, 1.6 μl of $MgCl_2$ (3 mM), 1 μl of forward primer (0.5 μM), 1 μl of reverse primer (0.5 μM), 2 μl of Fast Start DNA Master SYBR Green I and 5 μl of cDNA (equivalent to 40 ng of total RNA). The LightCycler experimental run protocol was as follows: denaturation (95 °C for 10 min), 45 cycles of amplification (95 °C for 15 s, 58–64 °C for 10 s, 72 °C for 25 s with a single fluorescence measurement). Quantitation of the PCR products was performed with the second derivative maximum method of the LightCycler software, using the external standard curve method. qRT-PCR products levels, which correspond to the transcript levels were normalized to those of *GAPDH*. All sample measurements were repeated at least three times and the results were expressed as the mean ± SD.

2.6. Protein extraction and western blotting

Proteins were extracted from the fibroblast cultures by homogenization in lysis buffer containing 1 mM sodium orthovanadate, 1% sodium dodecyl sulfate (SDS) and 10 mM Tris (pH 7.4). Subsequently, the homogenized protein samples were subjected to western blotting. The protein samples were electrophoresed on 10% SDS polyacrylamide gels and transferred to a polyvinylidene difluoride membrane (Bio-Rad Laboratories, Hercules, CA) by wet blotting. Then, the membranes

were blocked in TBS-T buffer containing 5% dry-milk (ECL™ Blocking Agent; GE Healthcare, Little Chalfont, UK) overnight at 4 °C. Immunostaining of the membranes was performed using several antibodies, each according to the manufacturer's instructions. Detection of the signals with Amersham™ ECL Plus Western Blotting Detection Reagents (GE Healthcare) was carried out using an LAS mini 3000 (Perkin-Elmer Life Sciences, Oak Brook, IL).

The following antibodies were used: mouse anti-SMN (BD Transduction Laboratories™, Franklin Lakes, NJ; 1:1000), mouse anti-splicing factor-2 (SF2/ASF) (Invitrogen Camarillo, CA; 1 μg/ml), mouse monoclonal anti-hnRNPA1 [4B10] (Abcam®, Cambridge, MA; 1:1000), mouse monoclonal anti-beta-actin (Abcam® Cambridge, MA; 1:1000) and peroxidase-linked sheep anti-mouse IgG (ECL, Amersham Biosciences; 1:5000). The intensity of the signals was determined using ImageJ (National Institutes of Health, Bethesda, MD; downloaded from http://rsbweb.nih.gov/ij/). The protein levels were normalized to those of beta-actin. All protein measurements were repeated at least three times and the results were expressed as the mean ± SD.

2.7. Statistical analysis

Statistical analysis of the data was performed using Microsoft Excel 2003 software and Statistical Package for the Social Sciences (SPSS Inc, Chicago, USA). Student's *t* test was conducted to evaluate the differences between groups. A probability of less than 0.05 was considered statistically significant. All data were expressed as the mean ± SD. Analysis of variance test was used to examine the differences between data obtained from the mock and VPA-induced cell cultures.

3. Results

3.1. Cytotoxicity analysis of VPA using a fibroblast cell line

We used the MTS assay to analyze the cytotoxicity of 10 mM VPA in the OK11 cell line after 0, 2, 4, 8, 16 and 24 h incubation with 10 mM VPA. The MTS assay measures survival and/or proliferation of cells [42].

As shown in Fig. 1, the 16 h and 24 h incubation with 10 mM VPA decreased cell viability by 14% and 17%, respectively. This suggests that the 16 h incubation with VPA at this concentration was not particularly toxic to the cell line. Based on these data, we incubated the cells for 16 h in all subsequent experiments.

3.2. VPA induces SMN expression

To confirm the effect of VPA on *SMN* gene expression [33,34], we compared the levels of VPA-induced

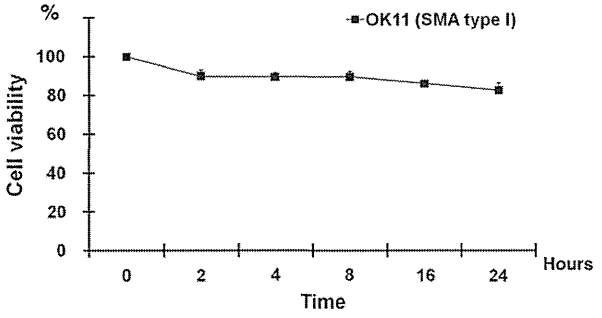

Fig. 1. Cytotoxicity analysis of VPA using the MTS assay. The cell viability of SMA type I fibroblast cell line (OK11) was measured after 0, 2, 4, 8, 16 and 24 h incubation with 10 mM VPA. The cell numbers decreased by only 14% and 17% after 16 h and 24 h incubation with VPA, respectively.

SMN transcripts and SMN protein levels with their respective baseline (mock status) levels in the cell lines, OK11, AM21 and CO31. The culture medium contained VPA at 0.05–10 mM. We measured the total-*SMN*, FL-*SMN* and Δ7-SMN transcript levels and SMN protein levels. Transcript levels were normalized to *GAPDH*, and protein levels were normalized to beta-actin.

The highest *VPA* concentration used in this study, 10 mM, induced the highest total-*SMN* and FL-*SMN* transcript levels in all three cell lines (Fig. 2a and b). The changes in total-SMN transcript levels from 0 to 10 mM of VPA were all statistically significant, at 0.29–0.75 in OK11, 0.44–0.78 in AM21 and 0.68–1.2 in CO31 (arbitrary units relative to GAPDH). The changes in FL-*SMN* transcript levels from 0 to 10 mM of VPA were also all statistically significant, at 0.21–0.51 in OK11, 0.38–0.83 in AM21 and 0.75–1.6 in CO31. Notably, the VPA-induced total-*SMN* and FL-*SMN* levels were similar between OK11 (SMA type I) and AM21 (SMA type II), but that the VPA-induced total-*SMN* and FL-*SMN* levels in CO31 (control) were significantly higher than those in the SMA cell lines. Δ7-*SMN* transcript levels were also significantly increased with 10 mM VPA treatment in cell lines AM21 and C031 (Fig. 2c). However, no change in the ratio of FL-*SMN* to Δ7-*SMN* (FL/Δ7 ratio) was observed in any cell lines (Fig. 2d).

The baseline (mock status) levels of the total-*SMN*, FL-*SMN* and Δ7-*SMN* transcripts in the SMA type I fibroblast cell line, OK11, were significantly lower than those in the SMA type II fibroblast cell line, AM21 (Fig. 2). These baseline *SMN* levels may reflect the differing copy number of the *SMN*2 gene among the cell lines. However, during VPA treatment, the increases in the transcript levels in OK11 and AM21 were similar to each other, which does not reflect the copy number.

To determine the SMN protein levels, we performed western blotting with a monoclonal antibody directed against the amino-terminus of the SMN protein.

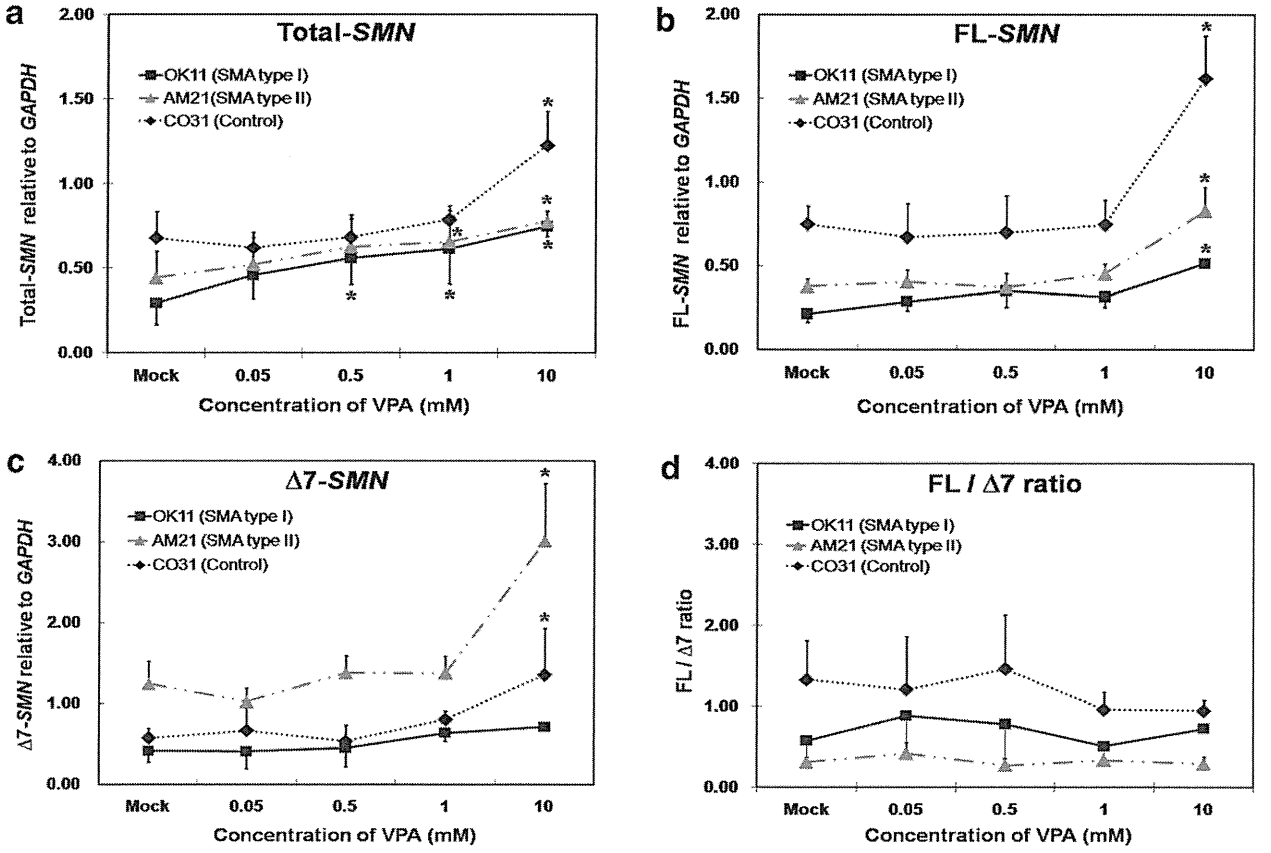

Fig. 2. Quantitative analysis of *SMN* transcripts. Upregulation of *SMN* transcript levels determined by quantitative real-time PCR in the cell lines, incubated for 16 h with different concentrations of VPA. All data are expressed as mean ± SD in arbitrary units relative to *GAPDH*. (a) Total-*SMN*. (b) FL-*SMN*. (c) Δ7-*SMN*. All SMN transcript levels reached their maximum at the highest VPA concentration, 10 mM. $^{*}p < 0.05$ *vs.* the baseline (mock). (d) The calculated FL/Δ7 ratios showed nearly unchanged levels, suggesting no effect on *SMN2* splicing after treatment with up to 10 mM VPA for 16 h.

Because the Δ7-SMN protein is essentially undetectable by western blotting [43], the SMN protein that we detected in this study was mainly FL-SMN protein. As shown in Fig. 3a, western-blotting revealed a slight increase in SMN protein expression in all three cell lines. The changes in SMN protein levels upon treatment with

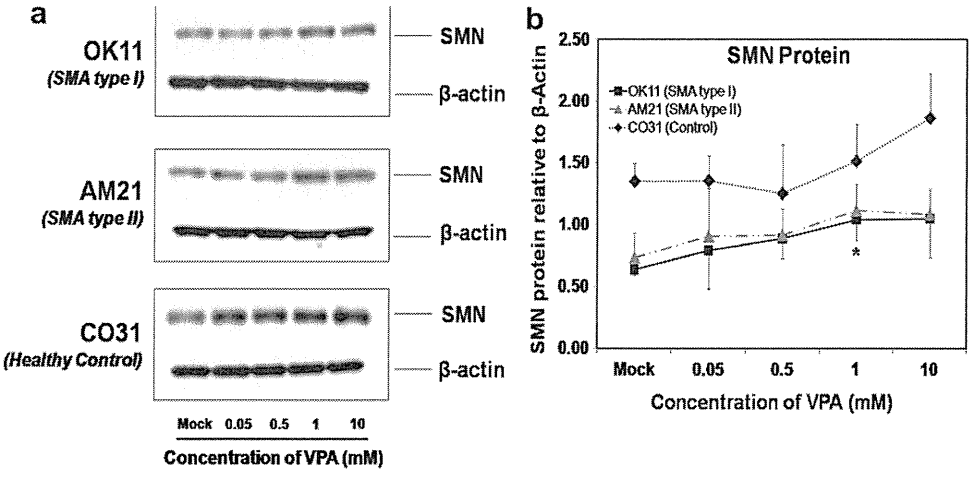

Fig. 3. Quantitative analysis of SMN protein. (a) Representative western blotting data illustrating the increase in SMN protein levels with VPA concentration. (b) Upregulation of SMN protein levels determined by western blotting in the cell lines, incubated for 16 h with different concentrations of VPA. The data are expressed as mean ± SD in arbitrary units relative to beta-actin. Densitometry revealed a 1.5-fold increase in SMN protein at 1 and 10 mM VPA relative to the baseline (mock) levels. $^{*}p < 0.05$ *vs.* the baseline (mock).